IV Meeting on Astrophysical Spectroscopy -

A&M DATA - Atmosphere

May 30 to June 2, 2022, Fruška Gora, Serbia

BOOK OF ABSTRACTS AND CONTRIBUTED PAPERS

Edited by Vladimir A. Srećković, Milan S. Dimitrijević,

Nikola Veselinović and Nikola Cvetanović

A&M DATA

UNIVERSITY OF BELGRADE | INSTITUTE OF PHYSICS | BELGRADE
NATIONAL INSTITUTE OF THE REPUBLIC OF SERBIA

Belgrade 2022

Scientific Committee

Local Organizing Committee

Organizers:

Institute of Physics Belgrade, Serbia,
Astronomical Observatory Belgrade, Serbia and
Faculty of Sciences – University of Novi Sad, Serbia

Text arrangement by computer: Tanja Milovanov

ISBN

Financially supported by the Ministry of Education, Science and Technological Development of Serbia

Production: Skripta Internacional, Mike Alasa 54, Beograd in 50 copies

SCIENTIFIC RATIONALE

Spectroscopy is a powerful tool for the analysis of radiation from different plasmas in astronomy, laboratory, fusion research, atmospheric research and industry. Effective theoretical analysis, synthesis and modelling of stellar spectra as well as the spectra from other plasma sources, depends on atomic data and their sources. In particular, for the modelling of stellar atmospheres and opacity calculations a large amount of atomic data is needed, since we do not know *a priori* the chemical composition of a stellar atmosphere. Consequently, the development of databases with atomic data and astroinformatics is important for stellar spectroscopy.

The Conference is planned as an opportunity to consider above mentioned aspects of spectroscopic research on plenary sessions and then to work on the special mini-projects, which will result in common papers to be published in international astronomical journals after the Conference.

Venue

Fruška Gora (Ceptor, Andrevlje), Serbia

CONTENTS

Curve fitting method of Stark width determination – example of H I line in G191-B2B spectrum

Zlatko Majlinger[1,2], Milan S. Dimitrijević[1] and Vladimir A. Srećković[3]

[1] Astronomical Observatory, Volgina 7, 11060 Belgrade 38, Serbia
E-mail: zlatko.majlinger@gmail.com, mdimitrijevic@aob.rs
[2] University of Zagreb, Faculty of Science (PMF), Croatia
[3] Institute of Physics Belgrade, UB, P.O. Box 57 11001, Belgrade, Serbia
E-mail: vlada@ipb.ac.rs

Astrophysical applications of Stark broadening theory were intensively developed in the last hundred years. For example, Verweij (1936) among the others pointed out the importance of Stark broadening influence on spectral line shapes even in the core of Balmer lines measured in the spectrum of the objects with log g > 5, e.g. white dwarfs. Since then, many scientific investigations have been done to prove significance of taking Stark width into consideration during spectral analysis of white dwarfs, even if the other elements have been investigated instead of hydrogen, where Stark broadening has affected more on wings than on the core of the spectral line. We propose here a simple curve fitting method for experimental determination of Stark width, using as an example of Ly β line in the spectrum of DA white dwarf G191-B2B. After comparison of our synthetic line with measured one, model of the white dwarf atmosphere can be used for determination of atmospheric depth where, according to our assumptions, the considered spectral line comes from originates.

Clear-sky spectral UV radiation modeling

Slavica Malinović-Milićević

Geographical Institute "Jovan Cvijić", Serbian Academy of Sciences and Arts,
Djure Jakšića 9, 11000 Belgrade, Serbia
E-mail: s.malinovic-milicevic@gi.sanu.ac.rs

Abstract

The parametric model NEOPLANTA was used to study the effects of various atmospheric conditions on terrestrial spectral UV irradiance. The capability of the model to correctly reproduce processes in the atmosphere is tested by changing input parameters such as ozone content, solar zenith angle, amount and type of aerosols, and altitude. The results of the model testing on input parameter change were satisfactory. As is expected, the amount of UV radiation reaching the surface is the most dependable on ozone layer thickness and solar zenith angle. Erythemal irradiance is more dependent on changes in the amount of ozone in the atmosphere than spectral UV irradiance, showing a significantly greater impact of UV-B radiation on human skin than radiation in the UV-A part of the spectrum.

Introduction

Although ultraviolet (UV) radiation (UVR) is a small part of the solar spectrum, its effect on the living world is very important because it is highly energetic and biologically very active. UVR is divided into the UV-C range (100–280 nm), UV-B range (280–315 nm), and UV-A range (315–400 nm). Surface UVR is predominantly within the UV-A range, while the UV-B wavelengths are largely filtered out by stratospheric ozone and make less than 5% of surface UVR. The UV-C radiation does not reach the earth's surface because it is completely absorbed in the upper atmosphere by ozone and oxygen. Besides ozone content, the ambient UVR depends on many other variables such as the position of the Sun, cloud cover, atmospheric aerosols type and content, surface albedo, and altitude. Processes are very complex since factors that control attenuation vary as a function of time and location.

The detection of the large depletion of stratospheric ozone in the last three decades of the 20th century (Molina and Rowland, 1974; Kaurola et al., 2000; etc) initiated increased public and scientific interest in the state of stratospheric ozone levels and variability of UV radiation and led to the establishment of the Montreal Protocol on Substances that Deplete the Ozone Layer in 1987. However, although mitigation activities over the past three decades significantly limited the production

of ozone-depleting substances and stabilized the ozone levels, UV radiation levels are still high (EEAP, 2019).

Although the ground-based UV monitoring network constantly growing since its formation in the 1980s, the measuring sites are still sparsely located, while UV data are, in most cases, limited to the period up to 25 years. Most of the stations are equipped with broadband meters (75% in Europe) that measures irradiance over a certain wavelength range and convert it into UV index, while the spectral measurement is even rarer (Schmalwieser, 2017). Due to lack of the long-term measurements different modeling techniques based on radiative transfer, and empirical method has been established (Diffey, 1977; Ruggaber et al., 1994, Mayer and Kylling, 2005, Lindfors and Vuilleumier, 2005; Rieder *et al.*, 2008; Paulescu *et al.*, 2010; etc). Radiative transfer models use available atmospheric parameters and estimate the UV radiation considering the scattering and absorption processes that take place in the radiation path through the atmosphere. In general, those models are more accurate than empirical, although their accuracy depends on the availability and reliability of input parameters.

This paper aims to improve our understanding of variations in the surface UVR using the parametric model NEOPLANTA which was developed at the University of Novi Sad (Malinović, 2003) as the first original model in Serbia.

Analysis and results

Description of the model

The numerical model NEOPLANTA calculates the intensity of clear sky direct and diffuse solar UVR, the corresponding erythemal UVR, and the UV index on the horizontal surface. The calculation of direct and diffuse UVR was performed with a wavelength resolution of 1 nm in the range of 280-400 nm. The model simulates the effects of the absorption of the UVR by O_3, SO_2, and NO_2, and absorption and scattering by aerosol and air molecules in the atmosphere. It calculates the spectral irradiance for a given solar zenith angle (SZA), but there is also the possibility of calculating the UV index for the whole day at intervals of half an hour from sunrise to sunset. It is designed so that it can be used in any location in the world at any time.

In the model, the atmosphere is divided into parallel layers (maximum 40), and it is assumed that each layer is a homogeneous medium with constant meteorological parameters. The vertical resolution of the model is 1 km for altitudes less than 25 km and 5 km for altitudes between 25 km and100 km, while the thickness of the last layer varies depending on the altitude. The values of the meteorological elements in each layer are determined using vertical profiles. The model contains data on the vertical profile of meteorological parameters of the standard atmosphere (Kurucz et al.,1984), but it is possible to use measured or modeled values. The influence of the surface on the intensity of UVR was calculated using the spectral albedo values for nine different types of surfaces.

The required input parameters are the local geographic coordinates and time or SZA, altitude, spectral albedo, and the total amount of gases. The model includes its vertical gas profiles (Ruggaber et al. 1994) and extinction cross-sections (Burrows et al. 1999; Bogumil et al. 2000), extraterrestrial solar irradiance shifted to terrestrial wavelength (Koepke et al. 1998), aerosol optical properties for 10 different aerosol types (Hess et al. 1998), and spectral albedo for nine different ground surface types (Ruggaber et al. 1994). Output data are spectral direct, diffuse, and global irradiance divided into the UV-A and UV-B part of the spectrum, erythemal irradiance, UV index (UVI), spectral optical depth, and spectral transmittance for each atmospheric component. All outputs are computed at the lower boundary of each layer.

The UV irradiance is calculated as the sum of the direct and the diffuse components. Calculation of the direct part of UVR is carried out by Beer-Lambert law. The direct irradiance $E_{dir}(\lambda)$ at wavelength λ received at ground level by unit area is given by:

$$E_{dir}(\lambda) = E_0(\lambda)T(\lambda), \quad (1)$$

where $E_0(\lambda)$ is the extraterrestrial irradiance corrected for the actual Sun-Earth distance and $T(\lambda)$ is the total transmittance that includes O_3, NO_2, SO_2, aerosol, and air transmittances. Each transmittance is calculated using optical depth $\tau(\lambda)$ is the product of extinction coefficient $\beta(\lambda)$ and ray path through the atmosphere s:

$$\mathrm{T}(\lambda) = exp[-\tau(\lambda)] = exp[-\beta(\lambda)s]. \quad (2)$$

The extinction coefficient of UV radiation, $\beta(\lambda)$, is calculated by the product of the cross-sectional area, $\sigma(\lambda)$, and layer particle concentration, N.

The diffuse UVR, $E_{dif}(\lambda)$, is divided into three components: (i) the Rayleigh scattering component, $E_{ray}(\lambda)$ (ii) the aerosol scattering component, $E_{aer}(\lambda)$ and (iii) the component that accounts for multiple reflections of irradiance between the ground and the air, $E_{rf}(\lambda)$. Calculation of $E_{dif}(\lambda)$ is made using an improved set of the equation described by Bird and Riordan (1986) and Blattner (1983) that were modified to include the wavelength range calculated by the NEOPLANTA model. The downward fraction is calculated from the same transmittance functions used to determine the direct UV irradiance. Calculation procedure of $E_{dif}(\lambda)$ is described in more detail in Malinović (2003) and Malinovic et al. (2006).

Evidence of an increasing number of skin cancer cases (IARC, 1992) has made it necessary to inform the public about the risk of solar radiation. Therefore, to take into account the potential erythemal effects of UVR on human skin calculated UV spectrum (in $Wm^{-2}nm^{-1}$) was multiplied by the erythema spectral weighting function ($s_{er}(\lambda)$) adopted by the CIE (CIE, 2019) thus providing the erythemal irradiance ($E_{er}(\lambda)$, in Wm^{-2}):

$$E_{er}(\lambda) = \int E(\lambda)s_{er}(\lambda)d\lambda, \quad (3)$$

where $E(\lambda)$ is spectral UV irradiance ($E_{dir}(\lambda) + E_{dif}(\lambda)$). $E_{er}(\lambda)$ assesses the potential of UV radiation to induce erythema (sunburn) and it is usually expressed as UVI ($UVI = E_{er} \times 40$). The erythemal irradiance accumulated over time gives the erythemal radiant exposure (H_{er}, in Jm^{-2}) (CIE, 2019).

Sensitivity of the model to input atmospheric parameters

Similar to measurements, models are subject to uncertainties that can be divided into two groups, numerical errors and uncertainties due to input parameters. Numerical errors can be avoided by programming and testing, while the uncertainties due to input parameters can be examined by sensitivity analysis and comparison with measured data.

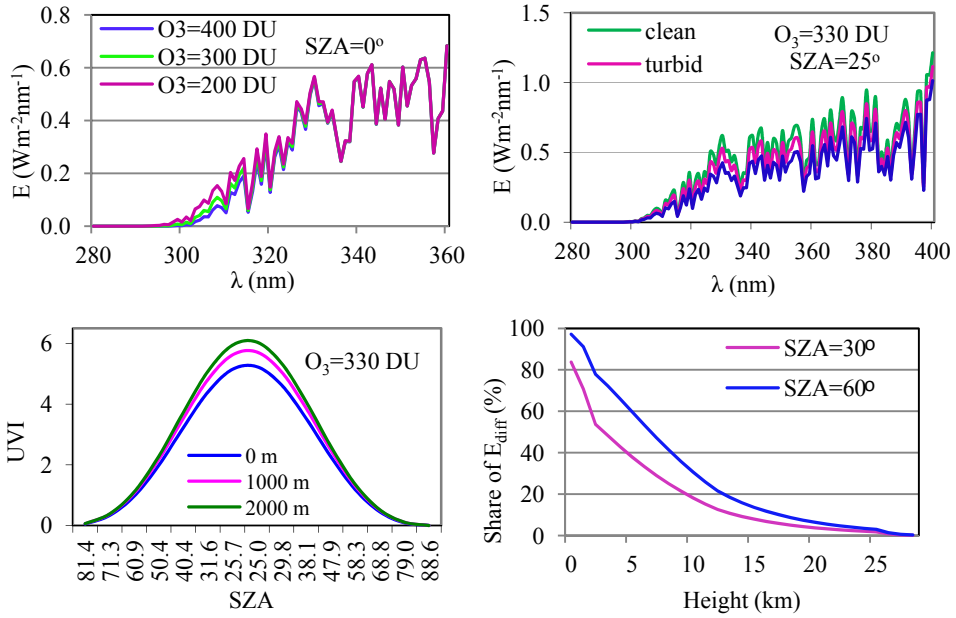

Fig. 1. Dependence of spectral UV irradiance on (a) ozone thickness and (b) air pollution levels; (c) dependence of UVI on altitude, and (d) dependence of share of diffuse UV irradiance on SZA.

All the input parameters of the model have an impact on the intensity of UVR reaching the surface, but not to the same extent. The capability of the model to correctly reproduce processes in the atmosphere is tested by changing input parameters. The tests have shown that the model can properly simulate changes in the intensity of UVR as well as the ratio of direct and diffuse UVR with the change in input parameters. The simulations qualitatively agree with the existing knowledge: (i) the intensity of UVR decreases with increasing the thickness of the ozone layer (Fig. 1a), the amount of aerosol (Fig. 1b), altitude, and the increase in

SZA (Fig. 1c), (ii) the contribution of diffuse UVR increases with increasing SZA (Fig. 1 d), the amount of aerosols, the presence of aerosols with a higher amount of water-soluble particles, air humidity, and more reflecting surface. Elevation of the surface above sea level has a small effect, but it becomes considerable in mountainous areas. Simulations have shown that ozone absorbs the largest amount of radiation while SO_2 and NO_2 have little impact, except in heavily polluted areas. It has been shown that aerosols can also greatly affect the amount and composition of UVR on the surface, while the effect on the surface reflection is small, except in the case of snow-covered areas. It has also been shown that the contribution of diffuse radiation in clear-sky UVR reaching the surface is large and that its amount depends mostly on SZA.

While extraterrestrial radiation $E_0(\lambda)$ is almost constant over time in UV-B and UV-A range $T(\lambda)$ transmittance is highly dependent on the composition of the Earth's atmosphere and is therefore very variable over time. However, as Fig. 1a shows, while $E_0(\lambda)$ is highly variable on the wavelength scale, the $T(\lambda)$ forms a relatively smooth curve. The processes in the Earth's atmosphere, mainly ozone absorption and Rayleigh scattering, vary smoothly with wavelength, define the transmittance $T(\lambda)$ and form the UV-B cutoff. The resulting spectrum $E(\lambda)$ in Fig. 2b is the product of graphs in Fig. 1a. Erythemal irradiance $E_{er}(\lambda)$ has a maximum in the wavelength range of 300 to 320 nm. $E_{er}(\lambda)$ and therefore it is more dependent on changes in the amount of ozone in the atmosphere than $E(\lambda)$, showing a significantly greater impact of UV-B radiation on human skin than radiation in the UV-A part of the spectrum (Fig. 2c).

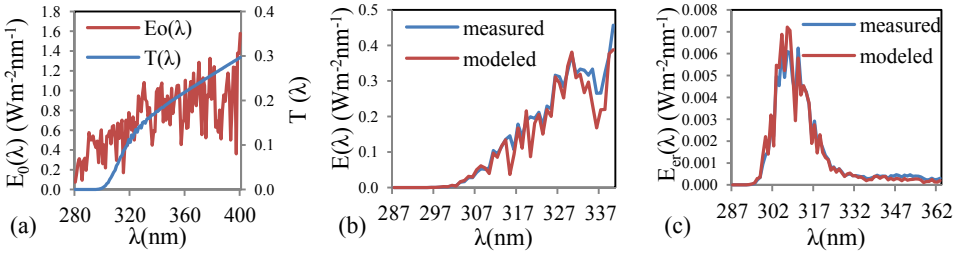

Fig.2. (a) Extraterrestrial UV spectrum$E_0(\lambda)$, and transmittance of the atmosphere $T(\lambda)$, (b) measured and modeled spectral UV irradiance $E(\lambda)$, and measured and modeled erythemal UV irradiance at 12:10 CET, 1 July 2021, Uccle, Belgium.

Conclusions

The parametric model NEOPLANTA was used to study the effects of various atmospheric conditions on terrestrial spectral UV irradiance. The capability of the model to correctly reproduce processes in the atmosphere is tested by changing input parameters such as ozone content, SZA, amount and type of aerosols, and altitude. Tests showed that the intensity of UVR decreases with increasing the thickness of the ozone layer, the amount of aerosol, altitude, and the increase in

SZA. It has been also confirmed that the contribution of diffuse UVR increases with increasing SZA, the amount of aerosols, the presence of aerosols with a higher amount of water-soluble particles, air humidity, and more reflecting surface. Elevation of the surface above sea level has a small effect, but it becomes considerable in mountainous areas. Erythemal irradiance is more dependent on changes in the amount of ozone in the atmosphere than spectral UVR, showing a significantly greater impact of UV-B radiation on human skin than radiation in the UV-A range. The results are in accordance with the existing knowledge.

References

Bird E.R., Riordan C., 1986, J. Clim. Appl. Meteorol. 25, 87–97.
Blattner W., 1983, Radiation Research Associates, Fort Worth, TX, 104 pp.
Bogumil K., Orphal J., Burrows J.P., 2000, Proc ERS- ENVISTAT Symp., Gothenburg, Sweden, ESA–ESTEC, pp 11
Burrows J.P., Richter A., Dehn A., Deters B et al., 1999, J. Quant. Spectrosc. Radiat. Transf. 61,509–517.
CIE, 2019, Erythema Reference Action Spectrum and Standard Erythema Dose; ISO/CIE 17166:2019 (E), CIE Standard. CIE Publications, Wien, Austria.
Diffey B.L., 1977, Phys. Med. Biol., **22,** 309–316.
EEAP, 2019, Nairobi: Environmental Effects Assessment Panel, United Nations Environment Programme (UNEP) 390 pp.
Hess M., Koepke P., Schult I., 1998, Bull Am Meteorol Soc 79, 831–844
IARC, 1992, Risks Hum., 1992, 55, 1–316.
Kaurola J., Taalas P., Koskela T., Borkowski J., Josefsson W. 2000, J. Geophys. Res., 105, 20813–20820.
Koepke P., Basis A., Balis D., Buchwitz M., et al., 1998, Photochem. Photobiol., 67,657–662
Kurucz R.L., Furenlid I., Brault J., Testerman L., 1984, National Solar Observatory Atlas No. 1
Lindfors A., Vuilleumier, L., 2005, J. Geophys. Res. 110, D02104.
Malinovic S., Mihailovic D.T., Kapor D., Mijatovic Z., Arsenic I.D., 2006, J. Appl. Meteorol. Climatol. 45, 1171–1177.
Malinović, S., 2003, M.S. thesis, University of Novi Sad, 103 pp.
Mayer B., Kylling A., 2005, Atmos. Chem. Phys., 5, 1855–1877.
Molina M.J., Rowland F.S., 1974, Nature, 249, 810–812.
Paulescu M., Stefu N., Tulcan-Paulescu E., Calinoiu D., et al., 2010, Atmos. Res. 96, 141–148.
Rieder H.E., Holawe F., Simic S., Blumthaler M., et al., 2008, Atmos. Chem. Phys. 8, 6309–6323.
Ruggaber A., Dlug R.,Nakajima T., 1994, J. Atmos. Chem., 18,171–210.
Schmalwieser A.W., Gröbner J., Blumthaler M., Klotz B., et al., 2017, Photochem. Photobiol. Sci., 16(9), 1349–1370.

Rate coefficients of He^+ ions in CF_4 gas

Željka D. Nikitović and Zoran M. Raspopović

Institute of Physics, University of Belgrade, Pregrevica 118, 11080 Belgrade, Serbia
E-mail: zeljka@ipb.ac.rs

This paper is dedicated to the presentation of the set of He^+ ions scattering cross-sections in CF_4 which is estimated using available experimental data for exothermic charge transfer cross-sections producing CF_3^+ and CF_2^+ ions and endothermic charge transfer cross-section producing CF^+, C^+ and F^+ ions. Due to significant particle losses, the experimental transport coefficients were not measured. The transport properties of He^+ ions in CF_4 required to model the discharge containing the mentioned ions were calculated by the Monte Carlo method at a temperature of T = 300 K. In this paper we give the characteristic energy and specially rate coefficients for low and moderately reduced electric fields *E /N* (*E*-electric field, *N*-gas density) and accounting for non-conservative collisions.

He-CF_4 mixtures are used in gas electron multipliers for various imaging purposes (X-rays, charged particles, thermal neutrons and dark matter detection) (Fraga M.M.F.R. et al. 2008). Bursts of electron multiplication affect production of various ions that may affect time distribution of detected particles (Bošnjaković D. 2016).

References

Fraga M.M.F.R., Fraga F.A.F., Fetal S.T.G., Margato L.M.S., Ferreira Marques R., Policarpo A.J.P.L., 2003, Nucl. Instrum. Meth. in Phys. Res. A 504, 88; Kaboth A., Monroe J., Ahlen S., Dujmić D., Henderson S., Kohse G., Lanza R., Lewandowska M., Roccaro A., Sciolla G., Skvorodnev N., Tomita H., Vanderspek R., Wellenstein H., Yamamoto R., Fisher P., 2008, Nucl. Instrum. and Meth.in Phys.Res. A 592, 63.

Bošnjaković D.,2016, Ph Dissertation, Faculty of Electrical Engineering, University of Belgrade, Belgrade, Serbia.

Stark broadening of Zn II spectral lines in stellar atmospheres

Milan S. Dimitrijević[1], Magdalena D. Christova[2], Nenad Milovanović[1] and Sylvie Sahal-Bréchot[3]

[1]Astronomical Observatory, Volgina 7, 11060 Belgrade, Serbia
[2]Department of Applied Physics, Technical University-Sofia, 1000 Sofia, Bulgaria
[3]LERMA, Observatoire de Paris, Sorbonne Université, Université PSL, CNRS, F-92190, Meudon, France

Broadening of spectral lines by interaction with electric microfield of charged particles, or Stark broadening is the most important pressure broadening mechanism for higher plasma temperatures and electron densities. Consequently, data for Stark broadening of different spectral lines are of importance for various plasmas in astrophysics, laboratory and inertial fusion investigations, for development and investigations of lasers and laser produced plasma research, modelling and diagnostics, as well as for plasmas in technology. Stark broadening data are especially needed and used in astrophysics, for abundance determinations, stellar spectra analysis and synthesis, stellar atmosphere modelling, opacity and radiative transfer calculations, determination of cosmic plasma parameters, and a number of other topics like stellar spectral type determination, modelling of subphotospheric layers, and monitoring of thermonuclear reactions in stellar interiors. Data on Stark broadenig of spectral lines are particularly needed for white dwarfs, because there, this is usually the principal pressure broadening mechanism. Atomic data for zinc, including Stark broadening, are often needed and for abundance determination of A and late B type stars. Zinc abundance determination for Galactic stars is important since the nucleosynthesis of this element is not well understood. Moreover, this is one of the key elements enabling to understand the star formation rate and chemical enrichment of the Galactic bulge. It is also important to probe the contribution of hypernovae at the lower metallicities during the bulge chemical enrichment process. Also, zinc can be observed in damped Lyman-α systems (DLAs), where, as the assumed proxy for Fe, it is of great importance for investigation of the chemical evolution of the Universe at high redshifts, by studying abundances in DLAs. The spectral lines of neutral and ionized zinc are observed in spectra of numerous stars of various spectral types. They are also of interest for modelling of subphotospheric layers and for radiative transfer calculations.

Stark broadening parameters of Zn II spectral lines have been measured several times. They are also calculated using the semiempirical and modified

semiempirical methods and estimated using regularities and systematic trends. We have calculated Stark broadening parameters, full widths at half intensity maximum and shifts for 34 multiplets of singly charged zinc ion, using the impact semiclassical perturbation formalism. Stark broadening parameters due to collisions with electrons, protons and helium ions have been obtained for a grid of electron densities and temperatures. The obtained results have been used to demonstrate the influence of Stark broadening mechanism on spectral lines of Zn II in stellar atmospheres. Stark widths and shifts for Zn II spectral lines will be also implemented in the STARK-B database (http://stark-b.obspm.fr/), which is a part of Virtual Atomic and Molecular Data Center (VAMDC - https://portal.vamdc.eu/vamdc_portal/home.seam). We note as well, that a link to STARK-B is in the Serbian Virtual Observatory (SerVO, http:servo.aob.rs).

Analysis of laser induced plasma plume in atmosphere: artificial neural network approach

Maja S. Rabasovic*, Bratislav P. Marinkovic and Dragutin Sevic

Institute of Physics Belgrade, University of Belgrade, Serbia

Time resolved analysis of spectra of laser initiated electric discharge spark in atmosphere is presented here. Spectral images of optical emission of atmospheric plasma are obtained by a streak camera.

Various machine learning (ML) techniques are used more and more for analysis of LIBS data. The combination of the popular machine learning algorithms (PCA and LDA, unsupervised and supervised techniques, respectively) with LIBS are used to complete rapid and precise classification of different samples (Bellou et al. 2020, Diaz et al. 2019, Pořízka et al. 2018, Yang et al. 2020, Zhang et al. 2020). An artificial neural network (ANN) algorithm is also used for the determination of electron temperature and electron number density in LIBS (Borges et al. 2014, D'Andrea 2015). The advantage of ANNs is in the possibility of reproducing nonlinear relations between the inputs and the output(s).

In our recent work we have combined several machine learning techniques, such as K-nearest neighbors classification together with clustering algorithms in supervised manner which is possible in SOLO software, in order to estimate plasma temperature (Rabasovic et al. 2022). Now, we have advanced research through the ANN and deep learning technique. Namely, large set of measured spectra are used to train the artificial neural network to obtain the estimation of plasma temperature. For machine learning approach to data analysis we use Solo+Mia software package (Version 9.0, Eigenvector Research Inc, USA) (Wise et al. 2006).

References

Bellou,E., Gyftokostas,N., Stefas, D., Odhisea, G.O., Courisa S., 2020, Spectr. Acta Part B: Atom. Spectr, 163, 105476. https://doi.org/10.1016/j.sab.2019.105746

Borges F., Cavalcanti G.H., Gomes G.C., et al., 2014, Appl. Phys. B, 117, 437–444. https://doi.org/10.1007/s00340-014-5852-8

Diaz, D., Molina, A., Hahn, D.W 2019, Appl. Spectrosc. 74 (1), 42–54. https://doi.org/10.1177/0003702819881444

D'Andrea E., Pagnotta S., Grifoni E., et al, 2015, Appl. Phys. B, 118, 353–360. https://doi.org/10.1007/s00340-014-5990-z

Pořízka P., Klusa J., Képeš E., Prochazka D., Hahn D.W., Kaiser J., 2018, Spectr. Acta Part B, 148 (2018) 65–82. https://doi.org/10.1016/j.sab.2018.05.030

Rabasovic M.S., Marinkovic B.P, Sevic D, 2022, Adv. In Space Res…in press... https://doi.org/10.1016/j.asr.2022.04.046

Wise, B.M., Gallagher, N.B., Bro, R., Shaver, J.M., Windig, W., Koch R.S., 2006. Chemometrics tutorial for PLS_Toolbox and Solo. ISBN: 0-9761184-1-6, Eigenvector Research, Inc. USA.

Yang, Y., Hao, X., Zhang. L., Ren, L., 2020, Sensors, 20 (5), 1393. https://doi.org/10.3390/s20051393

Zhang D., Zhang H., Zhao Y., Chen Y., Ke C., Xu T., He Y., 2020, Appl. Spectr. Rev. 57, 89-111. https://doi.org/10.1080/05704928.2020.1843175

Spatial variability of mineral dust single scattering albedo based on DREAM model

Maja Kuzmanoski[1], Luka Ilić[1,2] and Slobodan Ničković[3,1]

[1]Institute of Physics Belgrade, University of Belgrade, Pregrevica 118, 11080, Belgrade, Serbia
E-mail: maja.kuzmanoski@ipb.ac.rs
[2] Now at Barcelona Supercomputing Center, Barcelona, Spain
[3]Republic Hydrometeorological Service of Serbia (RHMSS), Belgrade, Serbia

Atmospheric aerosols have an impact on the Earth's radiation budget. They interact with solar and terrestrial radiation (direct effect) and play role in formation of clouds, thus modifying cloud properties and lifetime (indirect effect). Mineral dust is one of the most abundant aerosol types, with the largest contribution to global aerosol mass and significant optical depth (Kinne et al, 2006). There are still uncertainties in model estimates of dust radiative effects, partly due to variability in its mineral composition and shape of its particles, which are not accounted for in models (Boucher et al. 2013, Di Biagio et al. 2020). Single scattering albedo is an important parameter determining dust direct radiative effects, therefore its accurate representation in models is important. Dust single scattering albedo depends on its mineral composition, particularly on the content of iron oxide minerals (hematite and goethite).

In this study we present dust single scattering albedo values based on Dust Regional Atmospheric Model (DREAM) with incorporated particle mineral composition (Ničković et al. 2001, 2012). The domain of the model covers Northern Africa, Middle East and the European continent, with horizontal resolution of 1/5°. It uses eight particle size bins, in the radius range of 0.1-10 μm. DREAM model simulations of a dust episode that affected Mediterranean and part of Eastern Europe in June 2010 are performed to obtain total dust and hematite mass concentrations. Single scattering albedo is calculated using total dust and hematite concentration in each size bin from the model output. We analyze the spatial variability of the resulting dust single scattering albedo over the model domain. The results are evaluated using single scattering albedo values from Aerosol Robotic Network (AERONET) sunphotometer measurements (Holben et al., 1998).

References

Boucher, O., Randall, D., Artaxo, P., et al., 2013, IPCC 2013: Climate Change 2013: The Physical Science Basis, 571-657.

Di Biagio, C., Balkanski, Y., Albani, S., Boucher, O., and Formenti, P., 2020, Geophys. Res. Lett., 47, e2019GL086186.

Holben, B. N., Eck, T. F., Slutsker, I., et al., 1998, Remote Sens. Environ., 66, 1–16.

Kinne, S., Schulz, M., Textor, C., et al., 2006, Atmos. Chem. Phys., 6, 1815–1834.

Ničković, S., Kallos, G., Papadopoulos, A., and Kakaliagou, O., 2001, J. Geophys. Res., 106, 18113-18130.

Ničković, S., Vuković, A., Vujadinović, M., Djurdjević, V., and Pejanović, G., 2012, Atmos. Chem. Phys., 12, 845–855.

Lower Ionosphere perturbations due to Solar X-ray flares simultaneously monitored on two VLF signals with close GCPs

Aleksandra Kolarski and Vladimir Srećković

Institute of Physics, University of Belgrade, Pregrevica 118, 11000 Belgrade, Serbia
E-mail: aleksandra.kolarski@ipb.ac.rs

During Solar flare events, emitted energy from spectral range of X-rays plays the role of major source of additional ionization within atmospheric height range that corresponds to the sunlit lower Ionospheric heights (50-90 km). Thus triggered perturbations in subionospheric propagation of Very Low Frequency (VLF) radio signals, manifested as amplitude and phase delay deviations from their unperturbed values and from signal's regular behavior, reflect induced plasma perturbations due to incident Solar flare energy and are used for monitoring of the causative agent's characteristics and underlying coupling processes. Influence of relatively low to moderate intensity Solar flare events from second half of 23rd Solar cycle were analyzed, based on amplitude and phase delay perturbations of VLF signals transmitted from USA and UK and simultaneously monitored in Serbia and Hungary. Solar X-radiation data were taken from GOES satellites database. Numerical simulations were conducted by the use of Long Wave Propagation Capability (LWPC) software. Closely spatially positioned Great Circle Paths (GCPs) of VLF signals simultaneously observed at two receiver sites, enabled detailed comparative analysis regarding signals' behavior and extrema structure and redistribution along GCP during the influence of considered X-ray Solar flare events. Main results are presented in this paper.

Monitoring effects of low intensity X-ray Solar flares from 23/24 Solar cycle minimum on VLF signals recorded in Belgrade

Aleksandra Kolarski

Institute of Physics, University of Belgrade, Pregrevica 118, 11000 Belgrade, Serbia
E-mail: aleksandra.kolarski@ipb.ac.rs

D-region of the Ionosphere (50-90 km) is strongly under the influence of the Solar radiation from soft X-ray wavelength range (0.1-0.8 nm). As the consequence of incident Solar energy flux, Very Low Frequency (VLF) radio signals undergo perturbations, while transmit within Earth-Ionosphere waveguide. Based on registered VLF data, conditions within lower Ionosphere can be reproduced and electron density profiles can be obtained, by the use of the Long Wave Propagation Capability (LWPC) software and application of the Wait's theory. Effects of Solar flare events of low intensity (C and B class), in period from 2007 to 2011, during Solar minimum between 23rd and 24th Solar cycle were examined and monitored on VLF signals recorded in Belgrade (44.85N, 20.38W), at the Institute of Physics, Serbia. Solar X-ray radiation data were taken from GOES satellite database. Long Wave Propagation Capability (LWPC) software was used for numerical simulations of VLF signals' responses to analyzed X-ray Solar flare events. Main results are presented in this paper.

Numerical simulations of subionospheric VLF propagation under influence of moderate Solar X-ray flare events

Aleksandra Kolarski

Institute of Physics, University of Belgrade, Pregrevica 118, 11000 Belgrade, Serbia
E-mail: aleksandra.kolarski@ipb.ac.rs

Abstract

Soft X-ray radiation (0.1-0.8 nm) from Solar flare events, as one of the most important ionizing agents within D-region altitude range (50-90 km) of the sunlit lower Ionosphere, causes perturbations in subionospheric propagation of manmade Very Low Frequency (VLF) radio signals. Based upon VLF signal perturbations, by the use of the Long Wave Propagation Capability (LWPC) software relaying on Wait's theory, remote sensing of the lower Ionosphere from ground based stations is a well established research method. Subionospheric VLF propagation under influence of moderate Solar X-ray flare events (C and M class) during descending phase of the 23rd Solar cycle were analyzed on two VLF traces, simultaneously recorded by narrowband recording station in Belgrade (44.85N, 20.38W), Serbia. Influences of moderate Solar flares were inspected on one relatively short GQD/22.1 kHz and one relatively longer NAA/24 kHz VLF signal paths, with focus on numerical simulations of their propagation characteristics.

Introduction

The majority of ionospheric electron content lies within atmospheric thermosphere altitude range. Ionospheric layers significantly differ according to characteristics, constituents, variations, ionization processes involved etc. Ionospheric D-region is the innermost ionospheric layer, with the bulk of its electron content contained within altitude height range 50-90 km, within atmospheric mesosphere region. Since situated closest to the Earth’s surface, D-region is both influenced by the incident energy flux originated from Sun and outer space, and by the coupling with terrestrial processes. X-ray spectral range of Solar radiation penetrates deep into the Earth’s atmosphere and is one of the most important factors regarding the space weather. X-rays in wavelengths range 0.1-1 nm can reach heights with ionospheric D-region constituents, and thus are of the great importance as ionizing agent within this region during daytime. In quiet ionospheric conditions, production of electrons within D-region is mainly under

photoionization processes, UV Lyman-α spectral line 121.6 nm, EUV spectral lines ranging from 102.7 nm to 118.8 nm and galactic cosmic rays (e.g. Thomson et al. 2021 and references therein). Electromagnetic radiation during Solar flare events emitted in soft X-ray range (0.1–0.8 nm) causes photoionization of all neutral constituents within D-region and considerably exceeds ionization produced by regular factors (Lyman- α spectral line and cosmic rays), becoming a major ionization source in this region (Whitten and Poppoff 1965, Hargreaves 1992). Due to additional ionization, electron density within D-region increases, affecting the characteristics of the Earth-Ionosphere waveguide (Mitra et al. 1974).

Analysis and results

One of methods for investigating lower Ionosphere is utilization of manmade radio-signals in frequency range 3-30 kHz, belonging to the Very Low Frequency (VLF) range. These signals are globally emitted, usually by the military transmitters and for the military purposes, with stable signal and mainly in continual mode. This makes them very suitable for use in scientific purposes, as the remote sensing technique for monitoring of the lower Ionosphere. VLF signals transmit within Earth-Ionosphere waveguide, with stable amplitude and phase delay in quiet solar conditions (Budden 1988, Thomson 1993, McRae and Thomson 2000). Changes in electron density height profile within D-region, due to incident Solar X-ray radiation during solar flare events, influence propagation conditions within Earth-Ionosphere waveguide causing perturbations of VLF signals' amplitude and/or phase delay. Not only driven by Solar X-ray flares, VLF signal perturbations can also be driven by many other phenomena originating from extraterrestrial (e.g. γ-ray bursts, coronal mass ejections, solar eclipse etc.) to terrestrial (e.g. coupling with lightning activity, volcano eruptions, earthquakes, hurricanes etc.) environment. Many research groups dealt with topic of monitoring lower ionospheric features based upon the use of artificial VLF radio signals and their propagation characteristics (e.g. Silber and Price 2017 and references therein).

Utilization of Long Wave Propagation Capability (LWPC) numeric program package (Ferguson et al. 1998), based upon Wait's theory (Wait and Spies 1964, Wait 1970), and integrated with measured VLF data, has confirmed as successful technique for exploration of lower Ionosphere by many researchers (e.g. Thomson et al. 2011, 2005, McRae and Thomson 2000, 2004, Pal and Chakrabarti 2010, Basak and Chakrabarti 2013, Žigman et al. 2007, Grubor et al. 2008, Nina et al. 2011, 2012, 2018, Nina and Čadež 2014, Kolarski and Grubor 2014, 2015, Kolarski et al. 2011, 2022, Kumar and Kumar 2018, Šulić et al. 2016, Šulić and Srećković 2014, Srećković et al. 2021, Chowdhury et al. 2021 etc). Monitoring of ionospheric D-region during Solar flare events of moderate intensity from descending phase of the 23rd Solar cycle, as observed on two VLF signal traces simultaneously registered in Belgrade was conducted in this paper, with focus on numerical modeling procedure applied.

Influences of moderate intensity Solar flare events of C and M class, during descending phase of the 23rd Solar cycle, were analyzed on subionospheric VLF propagation on GQD and NAA VLF signal traces, as recorded in Belgrade (44.85N, 20.38E), at the Institute of Physics, by narrowband Absolute Phase and Amplitude Logger (AbsPAL) receiving station. GQD/22.1 kHz signal arrives from UK (Skelton (54.72N, 2.88W)) along relatively short and mostly an overland propagation path (GCP_{GQD}=1982 km), from WNW-ESE direction towards Belgrade, while NAA/24 kHz VLF signal arrives from USA (Maine (44.63N, 67.28W)) along relatively longer and mostly an oversea propagation path (GCP_{NAA}=6540 km), from W-E direction towards Belgrade. Solar X-ray irradiance data are taken from the website of National Oceanic and Atmospheric Administration (NOAA), from Geostationary Operational Environmental Satellite (GOES) Network database, from link: https://www.ngdc.noaa.gov/stp/satellite/goes/index.html.

Numerical simulations of propagation characteristics along their GCPs, under influence of analyzed C&M class Solar flare events, were conducted using LWPC software package, based on real measured amplitude and phase delay VLF data in Belgrade. During simulation process, the goal was to obtain simulated data, to fit as close as possible, to real measured data. Numerical simulations of subionospheric VLF propagation were carried out in ionospheric conditions before the influence of observed Solar flare events, denoted as *preflare state*, during the time evolution of each observed flare's influence on monitored VLF signal propagation, with *flare state* denoting the moment that corresponds to maximal X-ray irradiance i.e. I_{Xmax} and in ionospheric conditions recovered after the influence of observed Solar flare events, denoted as *postflare state*.

According to the Wait′s theory, electron density *Ne* (m^{-3}) height profiles within the Earth-Ionosphere waveguide at the altitude z (km), are determined by pairs of parameters, denoted as reflecting edge *sharpness* β (km^{-1}) of the lower boundary of the Ionosphere and *reflecting height H′* (km). Based upon exponential model of the Ionosphere, incorporated into LWPC software, unperturbed daytime ionospheric conditions are defined by parameter pair (β, *H′*) being held constant (0.3, 74) along entire propagation path. Perturbed ionospheric conditions are reproduced by modeling parameter pairs (β, *H′*) along propagation path, as manually entered values into REXP subroutine, with goal to get program's output amplitude and phase delay values as closest as possible to real measured VLF data at the receiver site. For purposes of obtaining *Ne* (m^{-3}), relation designed for daytime Ionospheric conditions based on Wait′s theory, was used:

$$Ne(z, H', \beta) = 1.43 \cdot 10^{13} \cdot e^{-0.15H'} \cdot e^{(\beta-0.15)(z-H')}. \quad (1)$$

Some of the numerically modeled parameters for subionospheric propagation of NAA and GQD signal traces for analyzed Solar flare events are given in Table 1, while electron density *Ne* (m^{-3}) height profiles in *flare states* are given in Fig. 1.

Table 1. NAA and GQD signal traces modeled parameters for analyzed Solar flares

Analyzed Solar flare events	Date (y/m/d)	06/04/07	06/07/06	05/09/07	06/12/06
	TimeUT (hh:mm)	08:03	08:36	12:44	12:58
	Class	C9.7	M2.5	C9.6	C4.8
	I_{Xmax} (Wm^{-2})	$9.74\cdot10^{-6}$	$2.51\cdot10^{-5}$	$9.62\cdot10^{-6}$	$4.82\cdot10^{-6}$
preflare conditions	NAA GQD	regular	regular	perturbed	perturbed
Quiet day (y/m/d)	NAA GQD	06/04/08	06/07/05	06/09/10 05/09/08	06/11/24 06/12/08
$\beta_{preflare}$ (km^{-1})	NAA GQD	0.30 0.33	0.361 0.28	0.432 0.335	0.253 0.425
β_{flare} (km^{-1})	NAA GQD	0.50 0.45	0.545 0.455	0.57 0.385	0.315 0.53
$\beta_{postflare}$ (km^{-1})	NAA GQD	0.375 0.325	0.392 0.32	0.425 0.325	0.22 0.355
$H'_{preflare}$ (km)	NAA GQD	74 72.5	74.1 75	73.3 71	71.3 72
H'_{flare} (km)	NAA GQD	67 69	69 65.5	70 66.5	66.6 70
$H'_{postflare}$ (km)	NAA GQD	72 72.5	73 72	73.4 72	74.2 72.8
$Ne_{preflare}$(65km) (m^{-3})	NAA GQD	$5.60\cdot10^{7}$ $7.02\cdot10^{7}$	$3.12\cdot10^{7}$ $5.07\cdot10^{7}$	$2.31\cdot10^{7}$ $1.12\cdot10^{8}$	$1.69\cdot10^{8}$ $4.26\cdot10^{7}$
$Ne_{preflare}$ (75 km) (m^{-3})	NAA GQD	$2.51\cdot10^{8}$ $4.24\cdot10^{8}$	$2.57\cdot10^{8}$ $1.86\cdot10^{8}$	$3.88\cdot10^{8}$ $7.10\cdot10^{8}$	$4.74\cdot10^{8}$ $6.66\cdot10^{8}$
$Ne_{preflare}$ (80 km) (m^{-3})	NAA GQD	$5.31\cdot10^{8}$ $1.04\cdot10^{9}$	$7.39\cdot10^{8}$ $3.56\cdot10^{8}$	$1.59\cdot10^{9}$ $1.79\cdot10^{9}$	$7.94\cdot10^{8}$ $2.63\cdot10^{9}$
Ne_{flare}(65 km) (m^{-3})	NAA GQD	$3.07\cdot10^{8}$ $1.38\cdot10^{8}$	$9.42\cdot10^{7}$ $6.64\cdot10^{8}$	$4.82\cdot10^{7}$ $4.68\cdot10^{8}$	$5.04\cdot10^{8}$ $5.89\cdot10^{7}$
Ne_{flare}(75 km) (m^{-3})	NAA GQD	$1.02\cdot10^{10}$ $2.77\cdot10^{9}$	$4.89\cdot10^{9}$ $1.40\cdot10^{10}$	$3.22\cdot10^{9}$ $4.91\cdot10^{9}$	$2.62\cdot10^{9}$ $2.63\cdot10^{9}$
Ne_{flare}(80 km) (m^{-3})	NAA GQD	$5.84\cdot10^{10}$ $1.24\cdot10^{10}$	$3.53\cdot10^{10}$ $6.44\cdot10^{10}$	$2.63\cdot10^{10}$ $1.59\cdot10^{10}$	$5.98\cdot10^{9}$ $1.76\cdot10^{10}$
$Ne_{postflare}$ (65 km) (m^{-3})	NAA GQD	$6.04\cdot10^{7}$ $7.28\cdot10^{7}$	$3.62\cdot10^{7}$ $8.87\cdot10^{7}$	$2.35\cdot10^{7}$ $8.57\cdot10^{7}$	$1.10\cdot10^{8}$ $5.22\cdot10^{7}$
$Ne_{postflare}$ (75 km) (m^{-3})	NAA GQD	$5.73\cdot10^{8}$ $4.19\cdot10^{8}$	$4.07\cdot10^{8}$ $4.86\cdot10^{8}$	$3.67\cdot10^{8}$ $4.93\cdot10^{8}$	$2.22\cdot10^{8}$ $4.06\cdot10^{8}$

$Ne_{postflare}$ (80 km) (m^{-3})	NAA GQD	$1.76 \cdot 10^9$ $1.01 \cdot 10^9$	$1.37 \cdot 10^9$ $1.14 \cdot 10^9$	$1.45 \cdot 10^9$ $1.18 \cdot 10^9$	$3.15 \cdot 10^8$ $1.13 \cdot 10^9$

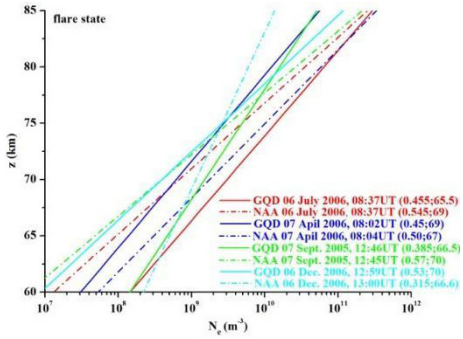

Fig. 1. Electron density height profiles for analyzed Solar flares in *flare states* for GQD and NAA signals, with corresponding modeled parameters (β, *H*′)

Conclusions

Conducted numerical simulations of subionospheric VLF propagation of GQD and NAA signals, based on Wait′s parameters and LWPC calculations, under the influence of chosen moderate C&M class Solar X-ray flare events from descending phase of the 23rd Solar cycle presented in this paper, are in good agreement with real measured VLF data at the place of the Belgrade AbsPAL receiver. It can be assumed, that numerically simulated average ionospheric conditions, held along GQD and NAA signal paths, realistically reproduce real ionospheric conditions, both for *preflare states* as for perturbed *flare states*, as well as for recovered *postflare states* in both waveguides and that applied modeling technique based on Wait′s theory and LWPC software utilization gives good modeling results for the purposes of qualitative analysis. Obtained results are in line with other studies performed by same technique for mid-latitude Ionosphere (e.g. Grubor et al. 2008, Žigman et al. 2007, McRae and Thomson 2004, Nina et al. 2012, Palit et al. 2013, Kolarski et al. 2015, 2022 etc.). Pattern, morphology and complexity of recorded signals' perturbations, forced by observed X-ray Solar flare events, differ for monitored GQD and NAA signal traces, since propagation differences within their waveguides, but also due to diurnal and seasonal ionospheric factors and X-ray Solar flare events' characteristics (Grubor et al. 2008). In general, GQD signal responds to soft Solar X-ray radiation of moderate intensity in more complex manner, with multiple amplitude and phase delay signal's extremes, compared to quite simple NAA response, with one maximum that corresponds to maximal X-ray irradiance. However, time delay Δt (Žigman et al. 2007) in signal reaching the maximum of X-ray Solar flare irradiance, for all analyzed cases, is up to 2 minutes.

Acknowledgments

Author thanks D. Grubor and D. Šulić. Thanks are due to The Ministry of Education, Science and Technological Development of the Republic of Serbia.

References

Basak, T., Chakrabarti, S. K., 2013, Astrophys. Space Sci., 348, 2, pp. 315–326.
Budden, K. G., 1988, The propagation of radio waves, Cambridge Univ. Press UK.
Chowdhury, S., Kundu S., Basak, T., Ghosh S., Hayakawa, M., Chakraborty S., Chakrabarti, S. K., Sasmal, S., 2021, ASR, 67, 1599–1611.
Ferguson, A. J., 1998, Computer program for assessment of long-wavelength radio communications, Version 2.0., Technical document 3030, Space and Naval Warfare Systems Center, San Diego CA 92152-5001, USA.
Grubor, D. P., Šulić, D. M., Žigman, V., 2008, Ann. Geophys., 26, 1731–1740.
Hargreaves, J. K., 1992, The solar-terrestrial environment, Cambridge Univ. Press.
Kolarski, A., Grubor, D., 2014, ASR, 53, 11, 1595 – 1602.
Kolarski, A., Grubor, D., 2015, J. Astrophys. Astr., 36, 4, 565–579.
Kolarski, A., Grubor, D., Šulić, D., 2011, Baltic Astron., 20, 591–595.
Kolarski, A., Srećković, V. A., Mijić, Z. R., 2022, Appl. Sci., 12, 582.
Kumar, A., Kumar, S., 2018, EPS, 70-29.
McRae, W. M., Thomson, N. R., 2000, JASTP, 62, 609–618.
McRae, W. M., Thomson, N. R., 2004, JASTP, 66, 77–87.
Mitra, A. P., 1974, Ionospheric effects of solar flares. Astrophysics and Space Science Library, vol. 46, D. Reidel publishing Company, Boston, USA.
Nina, A., Čadež, V. M., 2014, ASR, 54, 7, 1276-1284.
Nina, A., Čadež, V. M., Bajčetić, J., Mitrović, S. T., Popović, L. C., 2018, Sol. Phys., 293, 64
Nina, A., Čadež, V., Srećković, V. A., Šulić, D., 2011, Baltic Astron., 20, 609–612.
Nina, A., Čadež, V., Šulić, D., Srećković, V., Žigman, V., 2012B, Methods Phys. Res. B, 279, 106–109.
Pal, S., Chakrabarti, S. K., 2010, AIP Conf. Proc. 1286, 1, 42–60.
Silber, I., Price, C., 2017, Surv. Geophys., 38(2), 407–441.
Srećković, V. A., Šulić, D.M., Ignjatović, L., Vujčić, V., 2021, Appl. Sci. 11, 7194.
Thomson, N. R., 1993, JASTP, 55 (2), 173–184.
Thomson, N. R., Clilverd, M. A., Brundell, J. B., Rodger, C. J., 2021, J. Geophys. Res. Space Phys., 126, 10.1029/2020JA029043.
Thomson, N. R., Rodger, C. J., Cliverd, M. A., 2005, JGR, 110, A06306.
Thomson, N. R., Rodger, C. J., Clilverd, M. A., 2011, JGR, 116, 11305–11310.
Wait, R. J., 1970, Electromagnetic Waves in Stratified Media, Pergamon Press, Oxford, UK.
Wait, R. J., Spies, K. P., 1964, Characteristics of the Earth-Ionosphere waveguide for VLF radio waves, NBS Technical Note 300, USA.

Whitten, R. C., Poppoff, I. G., 1965, Physics of the Lower Ionosphere, Englewood Cliffs, N.J. Prentice-Hall, USA.
Šulić, D., Srećković, V. A, 2014, SAJ, 188, 45-54.
Šulić, D. M., Srećković, V. A., Mihajlov, A. A., 2016, ASR, 57, 1029–1043.
Žigman, V., Grubor, D., Šulić, D., 2007, JASTP, 69, 775–792.

Periodic variations of ionospheric Wait's parameters caused by changes in the intensity of incoming solar hydrogen Ly radiation

Aleksandra Nina[1], Vladimir Čadež[2], Luka Č. Popović[2,3,4] and Milan Radovanović[5,6]

[1]Institute of Physics Belgrade, University of Belgrade, Pregrevica 118, 11080 Belgrade, Serbia
E-mail: sandrast@ipb.ac.rs
[2]Astronomical Observatory, Volgina 7, 11060 Belgrade, Serbia
[3]Department of astronomy, Faculty of Mathematics, University of Belgrade, Studentski trg 16, 11000 Belgrade, Serbia
[4]Faculty of Science, University of Banja Luka, Bulevar vojvode Petra Bojovića 1A, Banja Luka, R. Srpska, Bosnia and Herzegovina
[5]Geographical Institute Jovan Cvijić SASA, Đure jakšića 9, Belgrade 11000, Serbia
[6]South Ural State University, Institute of Sports, Tourism and Service, Sony Krivoy street 60, 454080 Chelyabinsk, Russia

Abstract

Hydrogen Lyα photons corresponding to the 121.6 nm line in the solar spectrum are the most significant source of photo-ionization process in the D-region of the Earth's ionosphere. This radiation is continuously emitted and variations in its intensity in the ionosphere result from varying emission intensity of this radiation in the Sun and as well as from the Earth motion due to its rotation and revolution around the Sun. These changes affect variations in ionospheric parameters. In this paper, we analyse the variations of Wait's parameters which can further be used to determine the electron density and, consequently, more other ionospheric parameters in this region. Our analysis is based on the Quiet Ionospheric D-Region (QIonDR) model and shows the dependences of the observed parameters on the smoothed daily sunspot number, that represent variations in radiation during the solar cycle, and the day of year.

Introduction

Solar radiation is the main source of ionization in the Earth's ionosphere, and the most significant influence during calm conditions in the processes of photo-ionization in the lowest layer of this part of the atmosphere (D-region) has the hydrogen Lyα radiation. Consequently, this radiation plays a very important role

in the dynamics of electron density whose study is important for scientific analysis of ionospheric physical and chemical characteristics, and for practical applications, primarily related to the propagation of electromagnetic signals used e.g. in the fields of telecommunications and space geodesy.

One of the methods for determining the electron density is based on monitoring the ionosphere with very low/low frequency (VLF/LF) signals and using Wait's model of the ionosphere (Wait and Spies, 1964). This model is based on the assumption of a horizontally uniform ionosphere described by two independent parameters: the "sharpness", β, which describe the electron density vertical gradient, and the signal reflection height, H'.

In this paper, we provide an analysis of the influence of the incoming Lyα radiation in the observed part of the D-region on variations of Wait's parameters based on the QIonDR model (Nina et al., 2021).

Modelling

According to the QIonDR model, parameters β *and* H' can be calculated using the expression:

$$\beta = 0.2635 + 0.002573\sigma - 9.024 \cdot 10^{-6}\sigma^2 + 0.005351 \cdot \cos(2\pi(\xi - 0.4712)) \quad (1)$$

and

$$H' = 74.74 - 0.02984\sigma + 0.5705 \cdot \cos(2\pi(\xi - 0.4712) + \pi), \quad (2)$$

where σ and ξ are the smoothed daily sunspot number (over 21 days) and the seasonal parameter defined as DOY/365, where DOY is the day of year.

In this paper we analyse relative changes in Wait's parameters with parameter σ and DOY, d, according equations:

$$\frac{1}{\beta(i,j)}\frac{\Delta\beta(i,j)}{\Delta\sigma} = \frac{\beta(i+1,j)-\beta(i-1,j)}{2\beta(i,j)} \quad (3)$$

$$\frac{1}{H'(i,j)}\frac{\Delta H'(i,j)}{\Delta\sigma} = \frac{H'(i+1,j)-H'(i-1,j)}{2H'(i,j)} \quad (4)$$

$$\frac{1}{\beta(i,j)}\frac{\Delta\beta(i,j)}{\Delta d} = \frac{\beta(i,j+1)-\beta(i,j-1)}{2\beta(i,j)} \quad (5)$$

$$\frac{1}{H'(i,j)}\frac{\Delta H'(i,j)}{\Delta d} = \frac{H'(i,j+1)-H'(i,j-1)}{2H'(i,j)} \quad (6)$$

where i and j represent the i-th and j-th values of σ and DOY, respectively.

Results and discussion

The obtained results are presented in Figs. 1 (for changes of parameter β) and 2 (for parameter H').

The left panel of Fig. 1 shows relative variations of parameter β due to changes of sunspot number decrease with σ and they do not significantly change during the year. Contrary, the relative changes of this parameter in time are more pronounced with day than with σ. As one can see in the right panel of Fig. 1, the absolute values of the considered changes are the largest in the periods of equinox and at small sunspot numbers.

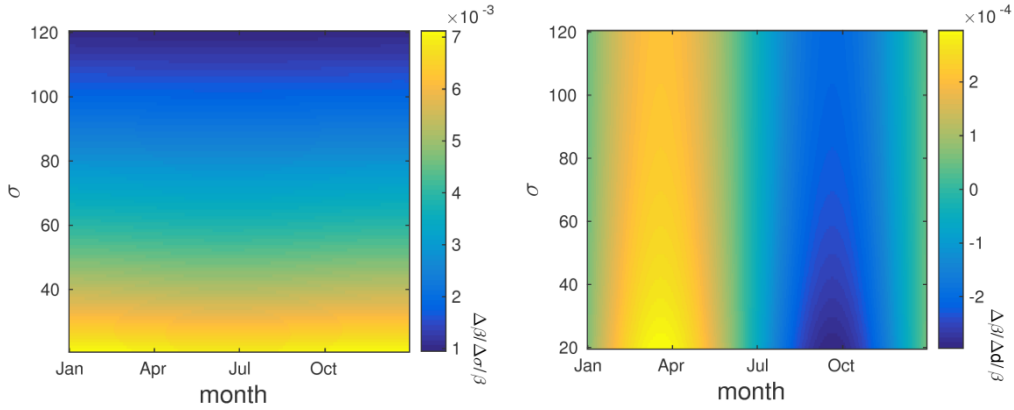

Fig. 1. Relative changes of Wait's parameter "sharpness", β, with changes of the smoothed daily sunspot number, $\Delta\sigma$ (left panel) and the day Δd (right panel) depending on the parameter σ and the day of year.

Relative changes of H' with changes of σ are more pronounced than the corresponding changes with days. As one can see in Fig. 2, the maximum changes in the first case are in the winter period, while the observed variations in the second case are most pronounced during the equinoxes.

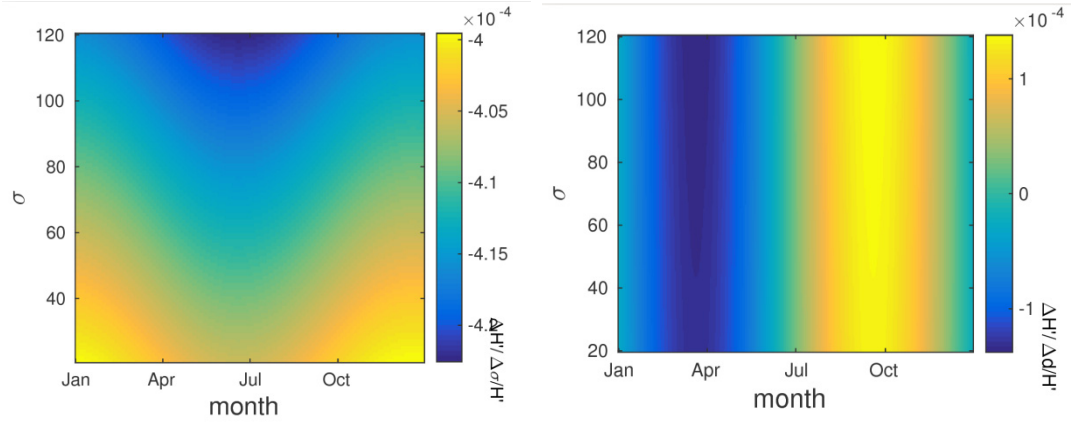

Fig. 2. Relative changes of Wait's parameter signal reflection height, *H',* with changes of the smoothed daily sunspot number, Δσ (left panel) and the day Δ*d* (right panel) depending on the parameter σ and the day of year.

Although the values shown are not large (they are of the order of 10^{-3} and 10^{-4}), they are continuous and cause noticeable disturbances for longer periods of several days or months, which may be significant for analyses of periodical changes in ionospheric characteristics.

Conclusions

In this paper, we present an analysis of the periodic changes in Wait's parameters caused by changes in the intensity of solar radiation and the Earth's revolution. The presented results were obtained by applying the Quiet Ionospheric D-region model, and they allow the following conclusions:

- Relative changes in the "sharpness" and the signal reflection height with the sunspot number reach the values of the order of per mille and tenth of per mille, respectively. In both cases they decrease with the sunspot number and the maximum values are reached during the winter solstice.
- The daily relative changes of both Wait's parameters are less than a per mille, their variations are more noticeable during the year than during the solar cycle, and they are most pronounced at equinox periods.

Keeping in mind that knowledge of Wait's parameters allows calculation of the D-region electron density and, consequently, modelling of several other ionospheric parameters, the impact of changes presented in this study on variations in ionospheric characteristics will be the subject of future research.

Acknowledgments

The authors acknowledge funding provided by the Institute of Physics Belgrade, Geographical Institute Jovan Cvijić SASA and Astronomical Observatory (the contract 451-03-68/2020-14/200002) through the grants by the Ministry of Education, Science, and Technological Development of the Republic of Serbia.

References

Nina, A., Nico, G., Mitrović, S.T., Čadež, V.M., Milošević, I.R., Radovanović, M., Popović, L.Č, 2021, Remote Sens., 13(3), 483.
Wait, J., R., Spies, K., P., 1964, Nat. Bureau Standards, Boulder, CO, USA.

GNSS signals as a tool for detection of the influence of solar radiation of terrestrial ionosphere

Oleg R. Odalović

Department of Geodesy And Geoinformatics, Faculty of Civil Engineering, University of Belgrade, Bulevar kralja Aleksandra 73, 11120 Belgrade, Serbia
E-mail: odalovic@grf.bg.ac.rs

Solar radiation has the most significant influence on photo-ionization in the Earth's ionosphere, and different parts of its spectrum in the UV and X domains have a dominant role in producing free electrons at different ionospheric heights. In calm conditions, the dominant role in photo-ionization processes in the D-region has the hydrogen Lyα line, while in the higher layers, the ionosphere is primarily ionized by photons from the X spectrum.

Through ionization processes, solar radiation significantly affects changes in the electron density in the ionosphere and, consequently, the propagation of electromagnetic (EM) waves in this atmospheric layer. One of the most significant EM waves propagating in the ionosphere is Global Navigation Satellite Systems (GNSS) signals with various applications, including navigation and positioning applications. Since 1987 International Association of Geodesy (IAG), as one of the several associations of the International Union of Geodesy and Geophysics (IUGG), has been responsible for establishing and maintaining European Terrestrial Reference System (ETRS). To establish and maintain ETRS, IAG has formed a special commission entitled EUREF (European Reference Frame), responsible for creating and maintaining the EUREF Permanent Network (EPN) as a science-driven network of continuously operating GNSS reference stations. More than 100 European agencies and universities are voluntarily involved in the EPN, with 368 stations all over Europe. In general, all GNSS stations continuously receive the data from all currently available GNSS: American NavStar, Russian GLONASS, Chines BeiDou, and European Galileo systems. The received data are stored in EPN Data Centres (DC), and all data are publicly available in several RINEX formats (Receiver Independent Exchange Format). Besides data centers, EUREF organized EPN Analysis Centers (AC) to provide products such as the EPN GNSS station positions and velocities, EPN zenith tropospheric path delay estimates, and ETRS89 satellite orbit and correction streams.

In the precise positioning process, the crucial element is modeling the ionosphere, which gives significance for practical applications to studies that analyze the influence of solar radiation and its spectrum on photo-ionization processes. Namely, the ionosphere delays EM waves that pass to it and induces a

delay of propagation related to the electronic density (Total Electron Content - TEC) and the wave frequency. This delay is directly proportional to the TEC and inversely proportional to the square of the carrier frequency. Those effects can produce an error in points coordinates from 3 to 15 m. Besides this effect, there are also effects caused by irregularities in the ionosphere – scintillation effects – which can cause a large number of cycle slips in GNSS signals. The magnitude of mentioned errors is the main reason for many studies and papers dedicated to modeling ionospheric effects on GNSS and using GNSS signals to determine global, regional, and local ionospheric models.

It is usual in GNSS applications to split the determination of ionosphere into deterministic and stochastic parts. The deterministic part is dedicated to creating models of the ionosphere, and the stochastic part is dedicated to the determination of short-term TEC variation throughout the estimation of Stochastic Ionosphere Parameters (SIP). This paper is dedicated to determining the deterministic part by modeling local, regional, and station-specific ionosphere models. All mentioned models are created based on available EPN data by Bernese GNSS Software Version 5.2 and mentioned models are represented by Taylor series expansion in the case of local models and spherical harmonic expansion for the regional and station-specific models. All models can be produced for the desired period and, in such a way, create relevant scientific data for studying the effect in the ionosphere induced by changes in solar radiation.

Influence of the periodic changes in the incoming solar hydrogen Ly-α radiation intensity on the total electron content in the ionospheric D-region

Dušan S. Petković[1], Oleg R. Odalović[1] and Aleksandra Nina[2,*]

[1]Faculty of Civil Engineering, University of Belgrade, Bulevar kralja Aleksandra 73, 11000 Belgrade, Serbia
[2]Institute of Physics Belgrade, University of Belgrade, Pregrevica 118, 11080 Belgrade, Serbia,
E-mail: sandrast@ipb.ac.rs

Abstract

This paper analyzes variations in the total electron content in the D-region induced by periodical changes in the solar hydrogen Lyα radiation. The considered changes are a consequence of variations in the solar radiation intensity during a solar cycle and a consequence of the Earth's revolution. The presented analysis is based on the Quiet ionospheric D-region (QIonDR) model, which shows the dependencies of ionospheric parameters on the smoothed daily sunspot number and season. We consider the vertical and slant (for different zenith angles) total electron content in the D-region (TEC_D) which are important for calculations of delays of satellite signals. The obtained results show a significant influence of the considered zenith angle and period of the solar cycle and season on calculating the considered ionospheric parameter.

Introduction

The ionosphere is an ionized part of the Earth's atmosphere that extends from approximately 60 km to 1000 km above the Earth's surface. Due to the high complexity of the ionosphere, the electron density is not uniform for all altitudes. Consequently, we can identify three ionospheric regions: D-, E-, and F-region.

The Earth's atmosphere, and therefore its ionized part, is permanently exposed to external (outer space) periodic and non-periodic influences. Some of the periodical effects have a significant role in complex chemical processes. Thus, variation in the solar hydrogen Lyα radiation has a dominant contribution to the free-electron production rate variation in photo-ionization processes in the D-region.

In this paper, we analyze periodical variations in the influence of the solar hydrogen Lyα photons on the production of the free electrons described by the D-region total electron content (TEC_D).

Total electron content modeling

The total electron content (TEC) is an ionospheric parameter characterized by the impact of the ionosphere's state on electromagnetic wave propagation. TEC represents the total number of electrons in a column with a 1 m^2 cross-section area along the signal path from a transmitter (satellite) to the receiver. TEC is expressed in Total Electron Content Units (TECU), which amounts to 10^{16} free electrons per squared meter.

TEC is usually calculated using appropriate models, such as the single-layer models (SLM) or multiple-layer models (MLM). SLMs assume that the ionosphere is a thin shell at a specific height (typical height value is between 300 km and 400 km). On the other side, MLMs consider numerous thin shells at specific heights instead of one thin shell.

Mathematically, TEC is defined by the following integral (Hofmann-Wellenhof et al., 2008, Seeber, 2003):

$$\mathrm{TEC}(t) = \int_S^R N_e dh, \tag{1}$$

where N_e stands for the electron density, h is the altitude, and S and R are the bottom and top ionosphere boundaries, respectively. Within the same spirit, for the top and bottom boundaries of the D-region, i.e., h_t = 90 km and h_b = 60 km, as limits of integration, the total electron content in the D-region, $\mathrm{TEC_D}$, can be expressed as:

$$\mathrm{TEC_D}(t) = \int_{h_b}^{h_t} N_e dh. \tag{2}$$

The previous equation stands for $\mathrm{TEC_D}$ determination if the signal path goes perpendicular to the D-region boundary, i.e., for 0° zenith angle. For other cases, the slant $\mathrm{TEC_D}$ ($\mathrm{STEC_D}$) is introduced based on the value of $\mathrm{TEC_D}$ and the corresponding mapping function $S(\theta)$ for the defined zenith angle θ:

$$\mathrm{STEC_D}(t) = S(\theta) \cdot \mathrm{TEC_D}(t) = \frac{\mathrm{TEC_D}(t)}{cos\theta}. \tag{3}$$

As we can see in Eq. (2), $\mathrm{TEC_D}$ can be determined based on N_e, which can be calculated using Wait's model of the ionosphere (Wait & Spies, 1964). This model assumes the horizontally uniform ionosphere described by two so-called Wait's parameters: the "sharpness" (β) and the signal reflection height (H'). N_e can be calculated according to expression (Thomson, 1993):

$$N_e(\beta, H', h) = 1.43 \cdot 10^{13} \cdot e^{-\beta(\sigma,\chi)H'(\sigma,\chi)} \cdot e^{[\beta(\sigma,\chi)-0.15]h}, \tag{4}$$

where Wait's parameters in the midday periods for the D-region above Central Europe can be determined using Eqs. (Nina et al., 2021):

$$H'(\sigma,\chi) = 74.74 - 0.02984\sigma + 0.5705cos(2\pi(\chi - 0.4712) + \pi), \quad (5)$$

and

$$\beta(\sigma,\chi) = 0.2635 + 0.002573\sigma - 9.024\cdot 10^{-6}\sigma^2 + 0.005351cos\big(2\pi(\chi - 0.4712)\big). \quad (6)$$

Here, σ and χ are the smoothed daily sunspot number and season parameter, which, multiplied by 365, deliver a day in a year, respectively. In these equations, β and H' are given in km^{-1} and km, respectively.

According to Eqs. (2) and (4), TEC_D can be determined using the expression (Todorović Drakul et al., 2016):

$$TEC_D(t) = 1000\frac{N_e(\beta,H',h_t) - N_e(\beta,H',h_b)}{\beta(\sigma,\chi) - 0.15}. \quad (7)$$

Analysis and results

In this contribution, we calculate TEC_D and $STEC_D$. Calculations are performed for 365 days and different values of σ in the range of 20 to 120 with a step equal to 20. TEC_D for all seasons and different values of σ are given in Fig. 1, where it is seen that TEC_D has maximal values in the period of the summer solstice and that increase with σ. The intensity of variations during a year increase with σ. The obtained values of TEC_D reach near 0.04 TECU.

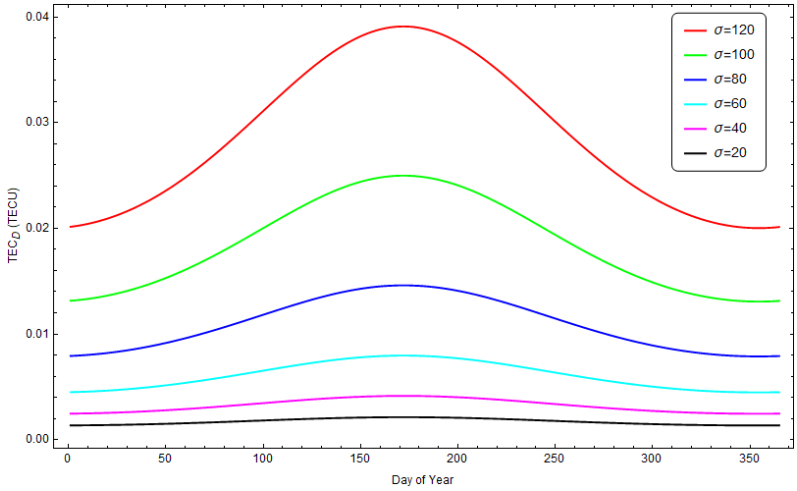

Fig. 1. Dependency of TEC_D on the day of the year for different σ.

$STEC_D$ is calculated based on TEC_D values and the zenith angle of 70°. Those results are given in Fig. 2, where one can see that the properties of the obtained dependencies are the same as for TEC_D.

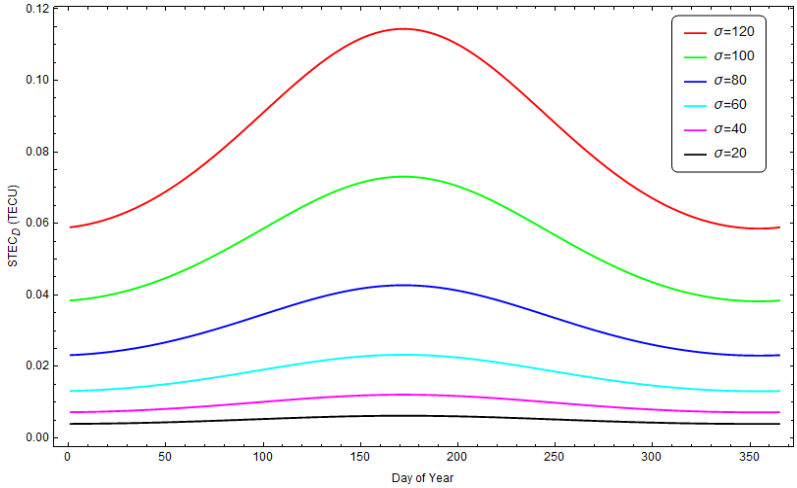

Fig. 2. Dependency of $STEC_D$ on the day of the year for $\theta = 70^o$ and different σ.

Comparisons of TEC_D and $STEC_D$ for the same σ are given in Fig. 3. Those comparisons show that $STEC_D$ has larger values than TEC_D for all values of σ, and that difference decrease with σ.

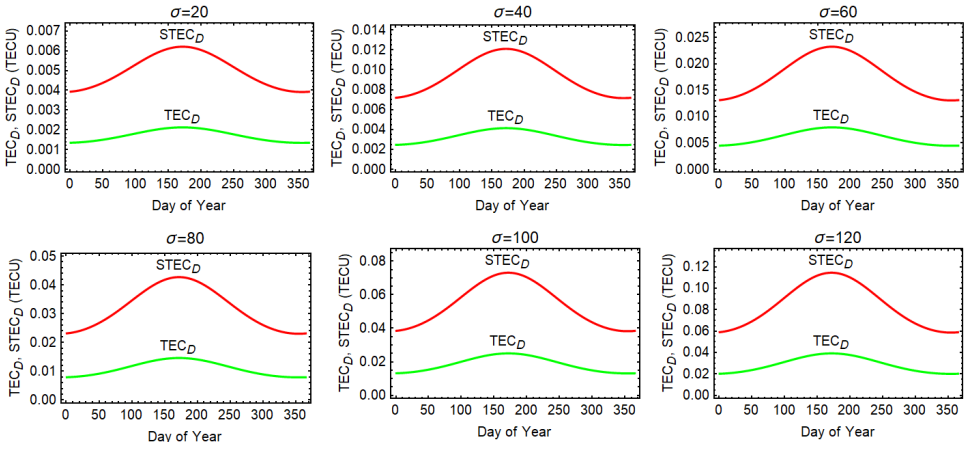

Fig. 3. Compared vertical and slant total electron content values in D-region over year for different σ values.

Conclusions

In this study, we present an analysis of the influence of variations in the intensity of the solar hydrogen Lyα radiation, arriving in the ionosphere on the D-region total electron content.

The obtained results show that the slant D-region total electron content has larger values than the corresponding vertical values. Furthermore, both quantities have maximal values during the summer solstice and increase with the sunspot number.

Acknowledgments

The authors acknowledge funding provided by the Institute of Physics Belgrade and the Faculty of Civil Engineering, University of Belgrade, through the Ministry of Education, Science, and Technological Development of the Republic of Serbia grants.

References

Hofmann-Wellenhof, B., Lichtenegger, H., Wasle, E., 2008, Springer, Vienna.

Nina, A., Nico, G., Mitrović, S.T., Čadež, V.M., Milošević, I.R., Radovanović, M., Popović, L.Č., 2021, Remote Sens., 13(3), 483.

Seeber, G., 2003, Walter de Gruyter, Berlin, New York.

Thomson, N.R., 1993, J. Atmos. Terr. Phys., 55, 173.

Todorović Drakul, M., Čadež, V.M., Bajčetić, J., Popović, L.Č., Nina, A., Serb. Astron. J. 2016, 193, 11.

Wait, J. R., Spies, K. P., 1964, National Bureau of Standards, Boulder, CO.

Approximation of the shape of hydrogen H_β spectral line with Voigt profiles

Z. Mijatović, S. Djurović, T. Gajo and I. Savić

University of Novi Sad, Faculty of Sciences, Department of Physics
Trg Dositeja Obradovića 4, 21000 Novi Sad, Serbia
E-mail: mijat@uns.ac.rs

Abstract

Stark broadening of hydrogen H_β line and good theoretical connection between its Stark halfwidth and plasma electron density favor it as one of the most reliable tools in plasma diagnostics. Problems occur when the Stark halfwidth has to be extracted from the measured halfwidth. Since the Stark profile cannot be described with an analytical function, the halfwidth extraction requires a very complicated deconvolution procedure. Results of attempt to apply two Voigt profiles to describe the shape of plasma broadened H_β line are presented. Instead of Voigt function, pseudo Voigt is used in this work. Obtained results are applied to experimental profiles and presented in the paper.

Introduction

The spectroscopic methods for determination of plasma electron densities are widely applied for both laboratory and astrophysical plasmas. Some of them are based on the Stark broadening of neutral and ion spectral lines where the halfwidths (width at half of line intensity FWH) and shifts are connected to the plasma electron density number. The observed line profiles emitted from plasmas are always resulted by the mutual action of different broadening mechanisms. Usually Stark broadening is dominant, but other mechanisms, like van der Waals, resonance, Doppler and instrumental broadening, can also have considerable contributions. The result is a profile that is the convolution of profiles caused by different broadening mechanisms. When Stark, Doppler and instrumental broadening are dominant over others, the resulting profile is the convolution of Stark (Lorentz) profile and Gaussian profile (Doppler and instrumental). The main difficulty is to extract the pure Stark profile, or, at least, Stark width, in order to obtain the plasma electron density. The situation is particularly complicated in the case of hydrogen Balmer spectral lines, especially for the H_β line. Theoretical profiles (Kepple et al. 1968, Vidal et al. 1973, Touma et al. 2000) of this line cannot be given in analytical form but in form of approximation (Gigosos et al. 2003) which, consequently, makes analytical deconvolution impossible. Therefore,

number of papers considered the possibility to apply the Voigt function in the deconvolution procedure (Ortiz-Mora et al. 2020, Olivero et al. 1977, Temme 2010). It was shown in (Konjević et al. 2012) that the use of one Voigt function for approximation of plasma broadened profiles of H_β is not appropriate at low plasma electron densities (bellow Fine structure limit – $4 \cdot 10^{13}$ cm^{-3}) nor at higher values (above Fine structure limit). This is quite expectable since H_β at higher electron densities is strongly asymmetric with two peaks of different intensities and a dip between them.

Procedures and results

Assumption in this work is that the components of H_β are concentrated in two groups forming two "profiles" with maximums approximately corresponding to the peaks of H_β. Under this assumption two Pseudo Voigt (PV) functions (NIST 2022) are used to fit the experimental profiles. PV is a linear combination of a Gaussian curve $G(x)$ and a Lorentzian curve $L(x)$ (instead of their convolution, which gives the Voigt function):

$$V_p(x,w) = \eta \cdot L(x,w) + (1-\eta) \cdot G(x,w) \text{ with } 0 < \eta < 1 \quad (1)$$

where w is the full width at half of maximum (FWHM) of PV profile. There are several choices for the parameter η. The next expression is accurate to 1 % (Ida et al 2000, Thompson et al. 1987):

$$\eta = 1.36603 \cdot (w_L/w) - 0.47719 \cdot (w_L/w)^2 + 0.11116 \cdot (w_L/w)^3 \,. \quad (2)$$

FWHM w is given as:

$$w = (w_G^5 + 2.69269 \cdot w_G^4 w_L + 2.42843 \cdot w_G^3 w_L^2 + \\ +4.47163 \cdot w_G^2 w_L^3 + 0.07842 \cdot w_G w_L^4 + w_L^5)^{1/5} \quad (3)$$

The fitting parameters should be I_1, w_{S1}, w_{G1}, l_{01} I_2, w_{S2},w_{G2} and l_{02} where I is used for intensity, w_L=w_S for Stark (Lorentz) width, w_G for Gaussian width and l_0 for peak positions. Fitting even one Voigt profile with all three parameters free, leads to overestimation of the Gaussian part (Konjević et al. 2012, also our experience). Fixing one of the parameters provide much better results (Konjević et al. 2012, our experience). Fortunately, in number of cases, the instrumental profile is Gaussian, resulting in instrumental width w_{Ins}. The plasma gas temperature can be measured in an independent way or can be estimated with a reasonably small error. Based on this fact, the Doppler width w_D, which is also Gaussian, can be calculated. The Gaussian width is $w_G = (w_{Ins}^2 + w_D^2)^{1/2}$ and can be considered as a known parameter. Secondly, the assumption is that both PV profiles have the same width w_S. This assumption is made because there is no reason why two fitting profiles would have different widths, since they are the subject of the same

electrical microfield. Now, the fitting parameters are I_1, I_2, l_{01}, l_{02} and w_S. The fitting code was written using *Mathematica*® package. This procedure was applied to more than 30 H_β line profiles recorded from plasmas of a wall stabilized arc (lower electron densities) and a T-tube (higher electron densities). The covered electron density range was $(1.3\text{-}76)\cdot 10^{16}$ cm-^{3} which is considerably more than one magnitude. Two examples of H_β line profiles, for low and high electron density, are presented in Figs. 1 and 2.

Reproducing the asymmetry and especially the dip of H_β has been always the problem in fitting procedures but, most of all, for theoretical calculations and modeling also. It can be seen from the presented figures that the fitted curves describe the profiles and the wings well, however the agreement in the center is not so good. If one is not interested to analyze the central part particularly, the rest of the fit is very useful for other considerations. Primarily, this fit enables the determination of the pure Stark width (because one of the fitting parameters is the Stark width) and, consequently, the extraction of the Gaussian part (if Stark, Doppler and instrumental broadenings are dominant). This is important if accurate Stark width is needed. Obtained results for other experimental H_β line profiles, used in this work, gave similar results, even at the highest plasma electron densities when the blue wing is considerably influenced by H_γ radiation.

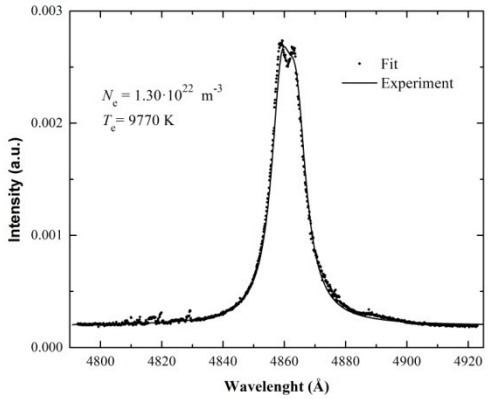

Figure 1. Experimental (wall stabilized arc) and fitted profiles at lower electron density.

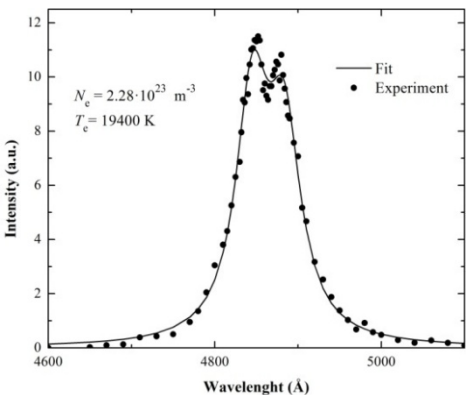

Figure 2. Experimental (T-tube) and fitted profiles at higher electron density.

Conclusions

In this work the Pseudo Voigt function was applied to fit experimental H_β spectral line in a wide range of plasma electron density values. The described method of fitting the H_β line profile enables to extract Stark halfwidth of the profile and gives the possibility for a more precise determination of the electron density.

Acknowledgments

This work was supported by the Ministry of Education, Science and Technological Development of the Republic of Serbia (Grant no. 451-03-9/2021-14/200125).

References

Gigosos, M. A., González, M. A., Cardeñoso, V., 2003, Spectrochim. Acta B, 58, 1489

Ida T, Ando M, Toraya H, 2000, Journal of Applied Crystallography 33, 1311.

Kepple P., Griem H. R., 1968, Phys. Rev. 173, 317.

Konjević, N., Ivković M., Sakan N., 2012, Spectrochim Acta B, 76, 16

NIST https://dlmf.nist.gov/7.19, May 2nd , 2022.

Ortiz-Mora, A., Díaz-Soriano, A., Sarsa, A., Dimitrijević, M. S. Yubero, C., 2020, Spectrochim. Acta B, 163, 105728.

Olivero J. J., Longgothum R. L., 1977, Journal of Quantitative Spectroscopy & Radiative Transfer 17, 233.

Temme N. M., in: Oliver Frank W. J. et al., (Eds.), NIST Handbook of Mathematical Functions, Cambridge University Press.

Thompson P., Cox D. E., Hastings J. B., 1987, Journal of Applied Crystallography 20, 79.

Touma J. E., Oks E., Alexiou S., Derevianko A., 2000, Journal of Quantitative Spectroscopy & Radiative Transfer 65, 543.

Vidal, C. R., Cooper, J., Smith, E. W., 1973, Astrophys. J. Suppl. Ser. 25, 37.

The study of atmospheric effects on cosmic ray muons in the Low Background Laboratory for Nuclear Physics at the Institute of Physics Belgrade

Mihailo Savić, Nikola Veselinović, Aleksandar Dragić, Dimitrije Maletić, Dejan Joković, Vladimir Udovičić, Radomir Banjanac and David Knežević

Institute of Physics Belgrade, University of Belgrade, Pregrevica 118, 11080 Belgrade, Serbia
Email: msavic@ipb.ac.rs

Galactic cosmic rays are being modulated in the heliosphere by different processes on the Sun. Upon arriving at Earth, they interact with nuclei in the atmosphere and produce secondary cosmic rays. Changing conditions in the atmosphere affect the propagation of secondary cosmic rays, especially the muon component. To increase the effectiveness of ground-based muon detectors these atmospheric effects need to be decoupled from non-atmospheric ones, and corrected for. To this end, in the Low Background Laboratory for Nuclear Physics at the Institute of Physics Belgrade, we are using several existing techniques but have also developed two new empirical methods for modeling and correction of barometric and temperature effects on cosmic ray muons. Newly developed methods proved to be equally or more effective than the most widely used ones. Such results allow for more precise study of solar modulation and more reliable long term monitoring of galactic cosmic ray flux, and could provide further insight into the relationship between atmospheric parameters and propagation of secondary cosmic rays in the atmosphere.

Data analysis on Serbian participation in COST Actions: Celebrating 50 years of research networks

Bratislav P. Marinković[a], Stefan Ivanović[b] and Zoran Mijić[c]

Institute of Physics Belgrade, Pregrevica 118, 11080 Belgrade, Serbia
[a]E-mail: bratislav.marinkovic@ipb.ac.rs Member of COST Committee of Senior Officials (CSO)
[b]E-mail: stefan.ivanovic992@gmail.com; data analyst
[c]E-mail: zoran.mijic@ipb.ac.rs; COST National Coordinator (CNC)

Abstract

Last year COST celebrated 50 years of the existence and successful networking activities. Although it does not finance the research itself, it already has become an inevitable part of each European country's community of researchers and innovators since it is devoted to both excellence and widening priorities of European Research Area. Here, we have briefly analyzed data of Serbian participation in COST Actions by tackling the issues of the rate and extent of involvement, presenting its interdisciplinary, organization of info-days and some success stories such as chairing the Actions.

Introduction

The European Cooperation in Science and Technology (COST) is the oldest intergovernmental funding organization in Europe created in the year 1971 with the aim to establish the research networks among scientists and innovators across Europe. Among 19 founding countries at that time there was Yugoslavia, whose researchers took active role in projects called *Actions*. In 2001, June 7th, Serbia (Federal Republic of Yugoslavia) rejoins COST and nowadays is one of 40 member countries together with one cooperating country that all form COST Association. Average number of countries participating in one Action was between 8 and 12 in the period of the first 20 years of COST establishment. Since then, this number is growing every year hitting the value of 31 and it is assumed to grow further in the forthcoming years (COST Brochure 2021).

COST organization experienced several transformations during its long history. It was established prior the start of Framework programs (FP), the first FP covering three years from 1984 to 1987. European Science Foundation, ESF, was an implementing agency via which EU financed COST organization from 2003

(Milutinović 2006). After the end of the 7th FP (2007-2013) and on the beginning of the Horizon 2020 (2014-2020), COST organization became COST Association, an entity functioning under Belgian law and directly financed by EU via Special Agreement. At the end of 2021 there were 289 running Actions, Serbian researchers participated in 93.8% (271) of them. In an Open Call for 2021 there were 22 638 proposers, among them 451 from Serbia, out of which 278 (61.6%) are female and 150 (33.3%) young researchers (COST Statistics 2021). They are called *secondary proposers* and they have a priority in the nomination for Management Committee (MC) of Action which has decision powers for governing of the COST Action in order to implement activities and manage the budget in the view of achieving the Action objectives.

Main decision body of COST Association is the COST Committee of Senior Officials (CSO) that forms the general assembly in which every country has two representative members. The COST National Coordinators (CNC) are the national contact points and they are responsible to appoint the national MC members to COST Actions. The COST Scientific Committee (SC) advises the COST Association about the Open Call, the procedures related to the submission, evaluation, and selection of proposals and it conducts the monitoring and final assessment of COST Actions. Serbian CNCs and CSO members were Prof. Dr Dragan Milutinović (2001-2006), Prof. Dr Biljana D. Stojanović (2006-2014), Prof. Dr Goran S. Đorđević (2014-2015), Dr Bratislav P. Marinković (2015-2021). At present Serbian CNC is Dr Zoran Mijić, CSO members are Dr B. P. Marinković and Ms Željka Dukić. Members of the SC are Prof. Dr Jovanka Lević (2013-2017) and Prof. Dr Viktor Nedović (2017-present).

COST info-days and COST connect events

A number of info-days have been organized in Serbia, where distinguished guests from COST have been participating, while the attendance of Serbian researchers always has been above 100 participants. These info-days have been always organized with the support of Ministry for Education, Science and Technological Development. The first info-day was organized by Prof. Dr Dragan Milutinović on 13th September 2001 with more than 300 participants. Mr Gösta Diehl, chairman of CSO, and Mr Erwin van Rij, head of COST Secretariat at the Commission of EU, visited "Vinča" institute and gave a presentation to an assembly of interested scientists at the Faculty of Mechanical Engineering (Milutinović 2006). On 14th March 2007 an info-day was organized by Prof. Dr. Biljana Stojanović (CNC and CSO member) and Ms Jasmina Milenković (CSO member). At this occasion a high delegation from COST was present: Prof. Dr Francesco Fedi, COST CSO President, Dr Martin Grabert, Director of COST office and Mr Peippo, Head of COST Secretariat-Council of the European Union. On September 2nd 2009 Prof. Dr Biljana Stojanović organized a seccesful info-day at which Prof. Dr. John G. Bartzis, Vice-President of CSO gave a lecture entitled

"COST: Past, Present and Future". On 25th March 2015, an info-day was organized with guests from COST, Dr. Ángeles Rodriguez-Peña, COST President and Ms Katalin Alföldi, Policy officer for excellence and inclusiveness of COST programme. The Serbian representation in 245 COST Actions within 9 Domains was summarized by Prof. Dr. Goran Đorđević, while the participant's experience was shared by Dr. Bratislav Marinković. During the info-day on 23rd March 2018 Acad. Sierd Cloetingh, COST President, Prof. Eva Kondorosi, Vice President of ERC and Chair of the Working Group on Widening European Participation, Mr Bart Veys, Policy officer and Mr Christer Halen, Policy administrator gave talks on COST, while Dr. Bratislav Marinković, Prof. Dr. Zorica Srdjević and Prof. Dr. Slobodan Cvejić presented Serbian experience in COST (https://mpn.gov.rs/vesti/u-rektoratu-univerziteta-u-beogradu-odrzan-cost-info-dan/).

On 10th October 2018 "COST Connect event" on *Sustainable Energy in the Danube Region* was held in Belgrade, organized by COST members Dr Ronald de Bruin, COST Director, Mr Bart Veys, Policy officer and Dr Elwin Reimink, Data and impact analysis officer, while the Serbian delegation was led by Prof. Dr Viktor Nedović, State secretary, Ms Željka Dukić, CSO member and Dr Bratislav Marinković, CNC and CSO member (https://mpn.gov.rs/vesti/u-beogradu-odrzana-konferencija-cost-connect/). COST Connect is a thematic event that brings COST Actions, policymakers and stakeholders together to exchange their ideas.

The info-day held on 29th March 2019 brought COST delegation (Dr Ronald de Bruin, Dr Elwin Reimink and Mr Christer Halen) in Belgrade. This info-day was combined with the presentations of Marie Skłodowska-Curie Actions, EURAXESS Serbia and EIT-Climate-KIC, European Institute of Innovation & Technology, while Serbian experience in COST was shared by Prof. Dr Bojan Blagojević from Faculty of Agriculture and Chair of COST Action CA18105 and by Dr Tijana Lainović from Medical Faculty, School of Dentistry, University of Novi Sad, MC member of COST Action CA16124. There was a large interest for this info-day at which 146 researchers participated.

Chairing COST Actions

The very first Chair of one COST Action was Prof. Dr Biljana Stojanović from the Institute for Multidisciplinary Research, University of Belgrade. She proposed the consorcium and chaired the Action 539 - Electroceramics from Nanopowders Produced by Innovative Methods (ELENA) which main objective was to improve the physical and electronic properties of advanced electroceramics and thick films produced by chemical, physical and mechanical synthesis techniques focusing on the polymeric precursors, sol-gel, spray pyrolysis, microemulsion, ultrasonic and freezedrying methods (Stojanović 2009). The Action started in 2005 and ended in 2009 with total number of 22 member and 6 non-COST countries involved. During the life of the Action there were organized 7 MC meetings, 11 working group (WG) meetings, 35 Short-term scientific missions (STMS), 7 Workshops and 2

Training Schools. More than 300 publications were published, while at the conferences more than 150 contributions were presented (Stojanović 2009).

During the first open call in 2018 the proposal by Prof. Dr Bojan Blagojević was successful and COST Action CA18105 - Risk-based meat inspection and integrated meat safety assurance (RIBMINS) was approved. The Action started in 2019 with the main aim to combine and strengthen European-wide research efforts on modern meat safety control systems. It will last till 2023, it is organized in 5 WG with researchers from 35 countries. This was the first time when Serbian institution holds a position of a Grant Holder.

The open call in 2019 was very productive, 3 of 45 Actions were approved in which the main proposer was from Serbia. Those Actions are: CA19110 - Plasma applications for smart and sustainable agriculture (PlAgri) with Dr Nevena Puač from the Institute of Physics Belgrade as a Chair; CA19128 Pan-European Network for Climate Adaptive Forest Restoration and Reforestation (PEN-CAFoRR) chaired by Prof Vladan Ivetić, Faculty of Forestry, University of Belgrade; CA19135 Connecting Education and Research Communities for an Innovative Resource Aware Society (CERCIRAS) chaired by Dr Gordana Rakić, Faculty of Sciences, University of Novi Sad. These Actions started in 2020 and will last 4 years.

The open call in 2020 brought one chairing position for Serbian scientist. It is the Action CA20108 FAIR NEtwork of micrometeorological measurements (FAIRNESS) proposed by Dr Branislava Lalić from Faculty of Agriculture, University of Novi Sad. The action intends to improve standardization and integration between databases/sets of micrometeorological measurements that are part of research projects or local/regional observational networks established for special purposes (agrometeorology, urban microclimate monitoring).

Success stories highlighted in the booklet on COST 50 years

One of the COST success stories is the Action TD1308 - Origins and evolution of life on Earth and in the Universe (ORIGINS). Prof. Didier Queloz, a member of this Action received Nobel prize in Physics in 2019 for discovery of ‘an exoplanet orbiting a solar-type star’. Serbian representatives in this Action that lasted from May 2014 till May 2018 were Prof. Dr Zorica Svirčev from University of Novi Sad, Faculty of Sciences and Dr Branislav Vukotić from Astronomical Observatory Belgrade.

In the special edition of COST booklet “*50 years of research networks*” (COST Brochure 2021) an article named “Doors Opening Across Europe Thanks to Tree Talk” highlights the research of Prof. Dr Saša Orlović, at the Faculty of Agriculture and Head of the Institute of Lowland Forestry and Environment at the University of Novi Sad and Dr Dejan Stojanović, also at the Institute of Lowland Forestry and Environment. In the article it has been pointed out how cross border collaboration is helping scientists in Serbia to open the doors of cooperation with their colleagues

around Europe. Prof. Dr Saša Orlović is a very active participant in COST Actions, being either MC member or MC substitue in nine past Actions (E42, E47, E52, FP0903, FP1106, FP1201, FP1204, ES1308, FP1403) and two running Actions (CA18134 and CA18201).

A testimony by Goran Tmušić, PhD student and research assistant at the Faculty of Sciences of the University of Novi Sad has been recorded by mentioning his experience as a participant of the COST Action CA16219 - *Harmonization of UAS techniques for agricultural and natural ecosystems monitoring* (https://50years.cost.eu/stories/goran-tmusic/). Member of MC of the Action CA16219 are Prof. Dr. Jasna Plavšić from the Faculty of Civil Engineering, University of Belgrade and Dr. Jugoslav Joković from the Faculty of Electronic Engineering, University of Niš.

The statement of Dr Ana Milojević from the Faculty of Political Sciences, University of Belgrade was posted at the COST website on the occasion of 50 years celebration: "All COST Actions are about getting people together. I collaborated with many excellent scholars, which I believe is one of the strongest points of COST". Dr Ana Milojević is MC member of CA17132 and MC substitute of IS1308 Action.

Analysis of Serbian participation in COST Actions

Involvement of Serbian researchers in COST Actions is constantly increasing as well as their share of total COST budget that is covering their activities. In 2020, Serbia participated in 270 Actions out of 291 Actions running at any time of the year (92.8%). In 2020, a total of 243 participants from Serbia were reimbursed by COST for their participation in COST Action networking activities (meetings, STSM, Training Schools) and our share in relation to the total budget of the Actions was 4.8% (in 2018 and 2019 these shares were 3.6%). In 2020, 58 participants from Serbia were involved in STSM, 34 trainees and 5 trainers were involved in Training Schools. There were also 12 Conference Grant participants from Serbia. In 2020, 45% of the participants from Serbia in networking activities holding a PhD were Early Career Investigators (ECI up to 8 years after obtaining PhD), while the average for all COST countries was 25% (COST Statistics 2021). However, the absolute figures for 2020 when compared to 2019 are significantly lower what is the consequence of covid-19 pandemic situation that reflected strongly on network activities.

Currently we are undergoing the statistical analysis of Serbian participation in COST Actions trying to achieve the how many of Serbian researchers and innovators have been participating in COST, how many of them have been in MC or at some other leading positions such as vice-chairs, WG leaders, STSM, grant awarding or science communication coordinators and Grant holder representatives.

The Actions that were approved in 2014 and before were distributed across different domains, each domain was covered by domain committee which could

approve certain number of Actions in proportion of the number of proposals. On the 163rd CSO meeting in Reading, UK, in November 2005 a decision of major restructuring of COST was taken. From June 2006 till 2014 there were 9 domains: Biomedicine and Molecular Biosciences (BMBS), Chemistry and Molecular Sciences and Technologies (CMST), Earth System Science and Environmental Management (ESSEM), Food and Agriculture (FA), Forests, their Products and Services (FPS), Information & Communication Technologies (ICT), Individuals, Society, Culture and Health (ISCH), Materials, Physical and Nanosciences (MPNS), Transport and Urban Development (TUD) and one Transdisciplinary Domain (TD). At that time, Serbia country rate participation in COST Actions was 21.9% out of 228 running Actions any time of the year (Annual Report 2006). The participation rates were 30.6% (of 222) (Annual Report 2007), 33.2% (out of 238) (Annual Report 2008), 32.2% (out of 255) in 2007, 2008 and 2009, respectively. In 2010 the percentage was 42% (Annual Report 2010). Participation of Serbian researchers was gradually but thoroughly increasing during the years: 50% of 301 Actions in 2012; 56% of 349 in 2013; 66% of 370 in 2014; 74% of 347 in 2015; 81% of 352 in 2016; 83% of 339 in 2017; 89% of 291 in 2018 and 92% of 292 in 2019 (COST Statistics 2020).

Interdisciplinary in COST research

Analysis of interdisciplinary of COST Actions is carried out in the view of 6 main OECD scientific fields, each field consists of several subfields. It covers the Actions from the period of open calls 2015-1 till the 2020-1. The summary result is given in Fig. 1. On the graph the first columns in blue represent data from the 7 open calls (2015-2018) while the second columns in grey are those from all 9 open calls (2015-2020). The methodology of representing data is the same as presented in (Marinković 2019). In every Memorandum of Understanding (MoU) it is mandatory to state to which scientific field and subfield the Action belongs to. Those data have been aggregated for each open call and results have been presented by the SC and COST data analysts. If the degree of interdisciplinarity of the proposals have been measured based on the key expertise defined in OECD Fields of Science and Technology (OECD DSTI/EAS/STP/NESTI(2006)19/ FINAL Document, 2007) selected by the main proposers when submitting the proposal, then the results show that almost half of all proposals are interdisciplinary, covering two, three or more disciplines. This interdisciplinary degree persists in COST open calls.

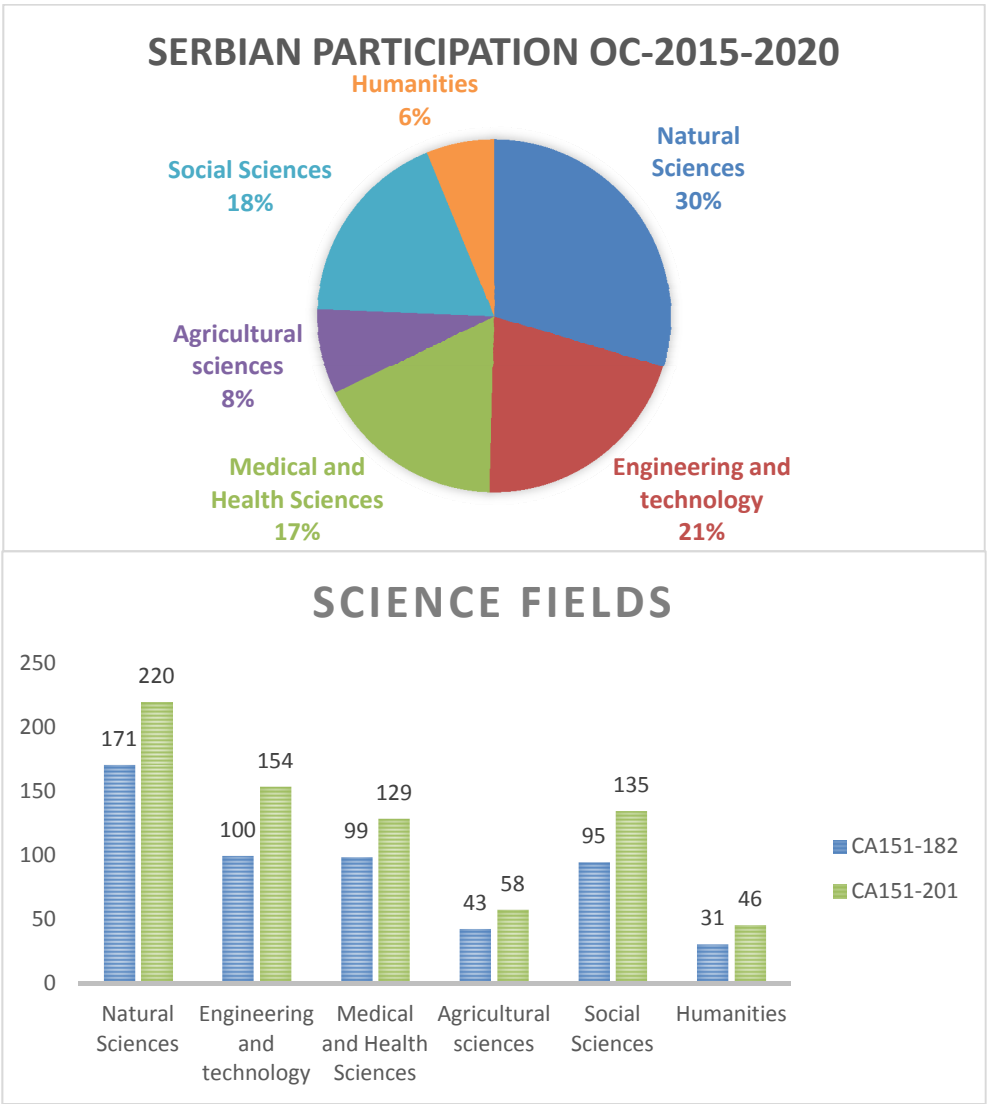

Fig. 1. Distribution of 6 main OECD scientific fields among Serbian research community in period 2015-2020: a) percentages; b) numbers in the first columns (blue) represent data from the 7 open calls (2015-2018), while the second columns (grey) are those from all 9 open calls (2015-2020).

Conclusions

Serbian participation in COST activities is significantly growing. We are taking part almost in all new Actions, e.g., in 39 out of 40 Actions launched in the latest open call OC-2020-1. That is showing the versatility of Serbian science and also its

incorporation into European Research Area (ERA). But it also shows that there are not enough national programs and calls that support research community. During covid-19 pandemic time (years 2020 and 2021) many traditional ways of research have changed and been transformed to adopt more distant access to facilities and networking. Also COST, on April 2021, launched new Virtual Networking Tools (VTNs) with two novel instruments, the Virtual Networking Support (VNS) Grant in order to stimulate virtual collaboration among the members of a COST Action, and the Virtual Mobility (VM) Grant(s) for strengthening the individual activities. The rules and principles related to the submission, running and monitoring COST Actions have been recently simplified together with the guidelines for COST Action Proposal Submission, Evaluation, Selection and Approval documentation (COST Documents and Guidelines 2022). Accordingly, the national rules for joining and proposing new Actions have changed. All changes have been presented at the national COST webpages (http://mail.ipb.ac.rs/~ncc-serbia/). The procedure for applying for the MC position can be finished by direct upload of the required documents via dedicated link (https://survey.ipb.ac.rs/index.php/666713?lang=sr). The great challenge is ahead our COST and research and innovation community to make a participation in new 70 Actions that are envisaged to be approved at the end of May 2022, together with the new 70 Actions within newest call OC-2022-1 that will be closed on 22nd October 2022. On the same time, it will be a great opportunity for Serbian science to be more extensively integrated in ERA.

Acknowledgments

Author thanks Profs. Drs Dragan Milutinović, Biljana Stojanović, Goran Đorđević and Ms Željka Dukić for useful comments and providing us with the relevant documentation. Thanks are due to the Ministry of Education, Science and Technological Development of the Republic of Serbia.

References

Annual Report, 2006, COST Association
Annual Report, 2007, COST Association
Annual Report, 2008, COST Association
Annual Report, 2010, COST Association
COST Brochure, 2021, 50 years of research networks, COST Association https://www.cost.eu/uploads/2021/05/COST_50-years_brochure-210503.pdf
COST Statistics, 2020, Serbia - Participation in COST Activities: Overview 2012-2019, COST Association
COST Documents and Guidelines, 2022, COST Association https://www.cost.eu/funding/documents-guidelines/
COST Statistics, 2021, Serbia - Participation in COST Activities: Overview 2020, COST Association

Marinković, B. P., 2019, "COST Actions as a wide network of researchers and innovators across Europe", Proc. The Seventh Conference on Information Theory and Complex Systems (TINKOS 2019), Belgrade 15-16 October 2019, Book of Abstracts, Eds. Ilić, V. and Mitrović Dankulov, M. (Mathematical Institute of the SASA and Institute of Physics Belgrade, University of Belgrade, Belgrade, 2019)

Milutinović, D., 2006, Report of the National COST Coordinator for the p eriod July 2001 to July 2006

OECD DSTI/EAS/STP/NESTI(2006)19/FINAL Document, 2007, Revised field of science and technology (FOS) classification in the Frascati Manual: https://www.oecd.org/sti/inno/38235147.pdf

Stojanović, B.D., 2009, COST Action 539 - Final Evaluation Report - Electroceramics from Nanopowders Produced by Innovative Methods (ELENA) 2005-2009 https://www.cost.eu/actions/539/

Rate coefficients and cross-sections for some collisional processes involving Rydberg atoms

Vladimir Srećković[1], Ljubinko Ignjatović[1], Milan Dimitrijević[2,3], Nikolai Bezuglov[4,5] and Andrey Klyucharev[5]

[1]Institute of Physics Belgrade, Pregrevica 118, 11080 Belgrade, Serbia
E-mail: vlada@ipb.ac.rs
[2]Astronomical Observatory, Volgina 7, 11060 Belgrade, Serbia
[3]LERMA, Observatoire de Paris, Université PSL, CNRS, Sorbonne Université, 5 Place Jules Janssen, 92190 Meudon, France
[4]Institute of Atomic Physics and Spectroscopy, University of Latvia, Riga, Latvia
[5]Saint Petersburg State University, 7/9 Universitetskaya nab., St. Petersburg, 199034, Russia

Processes of ionization which include highly excited atoms and molecules in various environments continue to draw attention of researchers because of their influence on the spectral characteristics of astrophysical and laboratory plasmas (Gnedin et al. 2009). Considered collisional ionization/recombination processes, which involve highly excited Rydberg atoms-RA(n) can influence on the ionization level and atom excited-state populations, and have a very significant influence on the optical properties. We obtained the cross-sections, as well as rate coefficients for potassium and sodium cases. The collisional data are obtained for wide range of parameters (500 K < T < 10 000 K) and principal quantum numbers up to 25. Our aim is to determine high quality data in order to be properly included in modern codes and databases for modelling geo-cosmic plasma, laboratory plasma, planetary atmospheres, ionosphere, etc. (Albert et al. 2020).

References

Albert, Damien, et al. "A decade with VAMDC: Results and ambitions." Atoms 8.4 (2020): 76.

Gnedin, Yu N., et al. "Rydberg atoms in astrophysics." New astronomy reviews 53.7-10 (2009): 259-265.

Low ionosphere modeling: new data and models

Vladimir Srećković[1], Veljko Vujčić[2], Aleksandra Kolarski[1], Jelena Barović[1,3] and Ognyan Kounchev[4]

[1]Institute of Physics Belgrade, Pregrevica 118, 11080 Belgrade, Serbia
E-mail: vlada@ipb.ac.rs
[2]Astronomical Observatory, Volgina 7, 11060 Belgrade, Serbia
[3]University of Montenegro, Podgorica, Montenegro
[4]Institute of Mathematics and Informatics, Bulgarian Academy of Sciences, Sofia, Bulgaria

Extreme radiation can cause addition ionization and alter the structure of the Earth's atmosphere. This kind of solar radiation and activity create sudden ionospheric disturbances (SIDs), induce various natural disasters, affect electronic equipment on the ground along with signals from space. Aim of this research is on the study of SIDs using very low frequency (VLF) radio signals in order to predict the impact of intense radiation on Earth and analyze ionosphere plasmas and its parameters (Srećković et al. 2022a). All data are recorded by VLF BEL stations and the model computation is used to obtain the daytime atmosphere parameters induced by this extreme radiation (Srećković et al. 2022b). We present new data, empirical model of the D-region plasma density and simple approximative formula for electron density.

References

Srećković, V. A., Šulić, D. M., Vujčić, V., Mijić, Z. R., & Ignjatović, L. M., 2021a, Applied Sciences, 11(23), 11574.
Srećković, V. A., Šulić, D. M., Ignjatović, L., & Vujčić, V., 2021b, Applied Sciences, 11(16), 7194

A&M Data: Processing and Modeling in Real Time

Veljko Vujčić[1] and Vladimir A. Srećković[2]

[1]Astronomical Observatory, Volgina 7, 11060 Belgrade, Serbia
E-mail: veljko@aob.rs
[2]Institute of Physics Belgrade, Pregrevica 118, Belgrade, Serbia

Atmospheric modeling requires usage of accurate radiative and collisional A&M data, both experimental and theoretical (Griem et al. 1962; Albert et al. 2020, Marinkovic et al. 2017a,b). From technological perspective, this often means heterogeneous e-ecosystem, consisting of different datasets and formats and various programming frameworks synchronized to work together, such as in Virtual Observatory (ivoa.net) or VAMDC (vamdc.org) project efforts. Understanding atmospheric processes is not only of pure scientific importance but for prevention of signal disturbances and infrastructure failures.

Our aim was to determine properties of the atmosphere i.e. lower ionosphere plasma in real time in order to establish a platform which can issue electronic alerts in a timely manner as well as show ongoing analytical overview of atmospheric properties (chemistry and physics). Moreover, it would enable real time modeling incorporating methods already introduced in flarED (Sreckovic et al. 2021a,b).

We selected data obtained from BLG ionospheric VLF (Very Low Frequency) station, and GOES satellite. For the initial development phase, we staged the data to behave as it would in a real-time scenario, by transforming input MATLAB data into a simulated stream of time series data. The analysis of VLF data was carried out simultaneously with the examination of the correlative solar X-ray fluxes collected from GOES satellite. Every data object obtained from these instruments can be regarded as an event, similar to a stock tick at the stock exchange. Correlation of some of these events leads to recognition of the events of higher order, and at the same time various kind of running statistics and analytics can be applied over the data. We used Esper, an open-source event-processing technology for the back-end.

We made a pre-alpha version of cep4vlf (Complex Event Processing for Very Low Frequency), which stages historical data in a real-time scenario. All work is available on GitHub (https://github.com/sambolino/cep4vlf). Purpose of cep4vlf is to enable automatic, real time detection of SID events, like flares, GRB's, lightning, etc. which can affect chemistry and physics of ionosphere. Moreover, it will enable real time modeling incorporating methods already introduced in flarED (https://github.com/sambolino/flared).

References

Albert, D.; Antony, B.; Ba, Y.A.; Babikov, Y.L.; Bollard, P.; Boudon, V.; Delahaye, F.; Del Zanna, G.; Dimitrijević, M.S.; Drouin, B.J.; Dubernet, M.-L.;et al., 2020 Atoms, 8, 76.

Griem, H. R., et al., 1962, Physical Review 125.1, 177.

Marinkovic, B. P., Bredehoft, J., Vujcic, V., Jevremovic, D., & Mason, N., 2017a, Atoms, 5, 46

Marinkovic, B. P., Jevremovic, D., Sreckovic, V. A., et al., 2017b, Eur. Phys. J. D, 71, 158

Srećković, V.A., Šulić, D.M., Vujčić, V., Mijić, Z.R. and Ignjatović, L.M., 2021a. Applied Sciences, 11(23), p.11574.

Srećković, V.A., Šulić, D.M., Ignjatović, L. and Vujčić, V., 2021b., Applied Sciences, 11(16), p.7194.

Ionosphere modeling and intense radiation

Vladimir Srećković[1], Jelena Barović[1,2] and Gordana Jovanović[2]

[1]Institute of Physics Belgrade, Pregrevica 118, 11080 Belgrade, Serbia
E-mail: vlada@ipb.ac.rs
[2]University of Montenegro, Podgorica, Montenegro

The perturbations in the Ionospheric D-region induced by solar flares were studied using monitored amplitude and phase data from Very Low Frequency (VLF) and Low frequency (LF) radio waves. The data were recorded by Belgrade stations system (Srećković et al. 2021a,b). The focus of this work is on the study of perturbed amplitude on VLF/LF signal caused by strong solar flares. Results show that the magnitude of the VLF perturbations is in correlation with intensity of X-ray. The model computations applied to obtain the electron density enhancement induced by intense solar radiation

References

Srećković, V. A., Šulić, D. M., Vujčić, V., Mijić, Z. R., & Ignjatović, L. M., 2021a, Applied Sciences, 11(23), 11574.

Srećković, V. A., Šulić, D. M., Ignjatović, L., & Vujčić, V., 2021b, Applied Sciences, 11(16), 7194

Collisional and radiative processes involving some small molecules: A&M data

Vladimir A. Srećković and Sanja Tošić

Institute of Physics Belgrade, Pregrevica 118, 11080 Belgrade, Serbia
E-mail: vlada@ipb.ac.rs, seka@ipb.ac.rs

Collecting necessary information on the different environments within our universe has become available with progress in observational astrophysics, experimental physics and computer modeling. Especially nowadays, atomic and molecular data and databases have become essential for developing models and simulations of complex physical/chemical processes and for the interpretation of (big)data provided by observations and measurements, e.g., laboratory plasma, planetary atmospheres, ionosphere, etc (Dubernet et al. 2016). It is necessary to constantly improve models by including as many processes as possible and using the most accurate data. This topic is very important because of existence of uncertainties on the rate coefficients for radiative and collisional processes and the need for accurate ones in order to be properly included in modern codes. Our aim is to determine high quality data. The main objective is to obtain, cross-sections and rate coefficients for some collisional and radiative processes, for conditions that exist in laboratory plasmas, planetary atmospheres, ionosphere, etc. (Albert et al. 2020).

References

Albert, D-, et al., 2020, Atoms 8.4, 76.
Dubernet, M. L., Antony, B. K., Ba, Y. A., et al.,. 2016, J. Phys. B, 49, 074003

Atomic structure and transition parameters of the V XVIII carbon-like ion

Lamia Abu El Maati[1], Mahmoud Ahmad[2,3], I. S. Mahmoud[2,4], Sahar G. Tawfik[5, 6], Najah Alwadii[7], Nabil Ben Nessib[8] and Milan S. Dimitrijević[9,10]

[1]Department of Physics, Faculty of Science, Benha University, Benha, 13513, Egypt
E-mail: lamia.aboelmaaty@fsc.bu.edu.eg
[2]Physics Department, College of Science in Zulfi, Majmaah University, 11952, Saudi Arabia.
E-mail: M.ahmad@mu.edu.sa
[3]Physics Department, Faculty of Science, Al Azhar University, 71524 Assuit, Egypt.
E-mail: M_ahmed@azhar.edu.eg
[4]Physics Department, Faculty of Science, Suez Canal University, Ismailia, Egypt.
E-mail: i.shaarany@mu.edu.sa
[5]Physics Department, Faculty of Science, Alexandria University, Egypt
[6]Department of Physics, College of Science, Princess Nourah Bint Abdulrahman University, P.O. Box 84428, Riyadh 11671, Saudi Arabia
E-mail: Sgmohamed@pnu.edu.sa
[7]Department of Physics, College of Sciences, King Khalid University, Saudi Arabia
E-mail: nalwadee@kku.edu.sa
[8]Department of Physics and Astronomy, College of Sciences, King Saud University, Saudi Arabia
E-mail: nbennessib@ksu.edu.sa
[9]Astronomical Observatory, Volgina 7, 11060 Belgrade, Serbia
E-mail: mdimitrijevic@aob.rs
[10]LERMA, Observatoire de Paris, Université PSL, CNRS, Sorbonne Université, 5 Place Jules Janssen, 92190 Meudon, France

The atomic and collisional parameters of carbon-like ions are significant for many important astrophysical quantities, such as the modeling of stellar atmospheres, the determination of stellar abundance, the analysis of spectral lines for laboratory plasmas or astronomical objects.

In this contribution, we calculated the energy levels and lifetimes of the carbon-like vanadium ion (V XVIII) using the atomic structure codes AUTOSTRUCTURE and GRASP2018. Weighted oscillator strengths and

transition probabilities are also calculated for the allowed transitions between the energy levels considered.

The calculations were carried out for the first 17 configurations: $2s^22p^2$, $2p^4$, $2s^22p3p$, $2s2p^23s$, $2s2p^23d$, $2p^33p$, $2s^22p4p$, $2s^23d^2$, $2s2p^3$, $2s^22p3s$, $2s^22p3d$, $2s2p^23p$, $2p^33s$, $2p^33d$, $2s^22p4s$, $2s^22p4d$ and $2s2p3d^2$.

Investigation of Laser Induced Breakdown Threshold

Violeta M. Petrović[1], Sanja D. Tošić[2], Hristina Delibašić Marković[1] and Ivan D. Petrović[3]

[1]Faculty of Science, University of Kragujevac, Radoja Domanovića 12, 34000 Kragujevac, Serbia
[2]Institute of Physics Belgrade, University of Belgrade, Serbia
E-mail: seka@ipb.ac.rs
[3]Technical Collage of Professional Studies Šumadia, Department in Kragujevac, Serbia

The phenomenon of laser-induced breakdown (LIB) in the air attracted great interest after the invention of the Ruby laser (see Damon et al. 1963). It occurs due to the interaction of the laser with a considered target when the laser pulse energy is greater than that of the binding electrons, involving different ways to create plasma. The initial step is photoionization (PI), which is followed by induced avalanche ionization (AI). As a result, a vast increase in the free electron density, $\rho(t)$, occurs. Usual way to describe their evolution is by the rate equation (see Vogel et al. 2005):

$$\frac{\partial \rho(t)}{\partial t} = \left(\frac{\partial \rho(t)}{\partial t}\right)_{PI} + \eta\rho(t) - g\rho(t) - \alpha\rho(t)^2.$$

The first two terms on the right side of the equation describe PI and AI rates, respectively, while the losses terms (due to diffusion $-g\rho(t)$ and recombination$-\alpha\rho(t)^2$) enter with a minus sign.

Even though LIB is a threshold-like process in terms of peak laser pulse strength (Polynkin et al. 2011, Shneider et al. 2012), defining the LIB threshold (LIBT) has long been recognized as an important challenge for developing methods that can produce trustworthy results.

Depending on the general-purpose, there are several types of evaluations that can be conducted to calculate the value of LIBT. For instance, according to Breischenk (2013), the portion of the laser pulse which initiates the plasma formation becomes equal to the LIBT.

The theoretical estimation of LIBT can be done by using the standard rate equation (see Keldysh 1964, Vogel 2005). According to Bekefi (1976) the LIBT in air, I_{th}, is given as:

$$I_{th} = \left(\frac{8\times10^2}{Pt_p\lambda^2}\right)(1 + 4.5\times10^{-6}P^2\lambda^2)\left(1 + 2\times10^8 Pt_p\right),$$

where P is pressure, while t_p and λ denote pulse duration and wavelength of the applied laser, respectively.

The validity of our calculations was tested by comparing the results of comprehensive propagation simulations with data from available experiments (Gao et al. 2019). Experimental results were satisfactory and gave good agreement to the presented model.

References

Bekefi, G. Principles of Laser Plasmas (John Wiley, New York, 1976)
Brieschenk, S., Kleine, H. and O'Byrn S., 2013, J. Appl. Phys. 114: 093101
Damon E. K. and Tomlinson R. G., 1963, Appl. Opt. 2, 546- 547
Gao, Z., Han, L. and Li, J., 2019, Pacific Rim Laser Damage 2019: Optical Materials for High-Power Lasers 11063, 1106305.
Keldysh, L.V., 1965. Zh. É ksp. Teor. Fiz. 47, 1945 1964 Sov. Phys. Jetp, 20, 1307
Polynkin, P. and Moloney, 2011, Appl. Phys. Lett., 99, 151103
Shneider, M.N. and Miles, R.B. 2012, Phys. Plasmas, 19, 083508
Vogel, A., Noack, J., Hüttman, G. and Paltauf, G.J.A.P.B., 2005, Applied physics B, 81(8), 1015-1047

Gravity satellite missions measurement data for atmospheric density estimation

Ljiljana M. Brajović[1] and Miodrag Malović[2]

[1]University of Belgrade, Faculty of Civil engineering, Bul. kralja Aleksandra 73, 11120 Belgrade, Serbia
E-mail: brajovic@grf.rs
[2]University of Belgrade, Innovation center of Faculty of Technology and Metallurgy, Karnegijeva 4, 11120 Belgrade, Serbia

Gravity satellite missions measurement data are primarily intended for use in the estimation of an accurate model of Earth's gravity field. The satellites' almost circular orbits with polar or near-polar inclination of the orbital planes, and low altitude (between 250 and 500 km), enable almost full coverage of the globe. Orbit tracking by precise high orbiting navigation satellite system provides the data about three-dimensional satellite position and its deviations. Precision accelerometers on the satellites extend the ability to monitor non-gravitational forces acting on them continuously. One of these forces, atmospheric drag along orbits, can be derived from the orbit track positions and their derivatives, and also from the precise accelerometer measurements, so it can be used for atmospheric mass density determination. On the other hand, the density of the atmosphere and its main constituents can be derived from the spectroscopic measurements. One of the examples is thermospheric mass density determination using neutral mass spectrometers on earlier satellite missions. Measurement of the Earth's far ultraviolet (FUV) dayglow is used to infer number density profiles of N_2, O, and O_2. Combination of accelerometers measurements and spectroscopic data is the foundation of two widely used empirical models of thermospheric mass density. This contribution describes the basic measurements on gravity satellite missions and atmospheric drag estimation, gives the comparison and combination of obtained data with spectrometric measurements of atmospheric density, and lists potential improvements using the data from the recently launched satellite gravity missions.

References

Bruinsma, S. L., Doornbos, E. , Bowman, B. R., 2014, Adv. Space Res., 54, 576.
Emmert, J. T., 2015, Adv. Space Res., 56, 773.
Flechtner, F., Reigber, C., Rummel, R. et al., 2021, Surv. Geophys. 42, 1029.
Siemes, C., Maddox, S., Carraz, O. et al., 2022, CEAS Space J.

van der Meijde, M., Pail, R., Bingham, R., et al., 2015, Int. J. Appl. Earth Obs. Geoinf., 35, 4.
Xiong, C., Lühr, H., Schmidt, M., Bloßfeld, M., et al., 2018, Ann. Geophys., 36, 1141.
Xu, T., Ren, L., & Gao, R., 2017, Geod. Geodyn., 8, 246.
Yu, T., Ren, Z., Yue, X., Yu, Y., & Wan, W., 2019, J. Geophys. Res. Space Phys., 124, 2165.

Absolute differential cross section for elastic electron scattering from halothane molecule at 150eV

Jelena B. Maljković[1], Jelena Vukalović[1,2], Zoran Pešić[3], F. Blanco[4], G. García[5] and Bratislav P. Marinković[1]

[1]Institute of Physics Belgrade, University of Belgrade, Pregrevica 118, 11080 Belgrade, Serbia
E-mail: jelenam@ipb.ac.rs
[2]Faculty of Science, University of Banja Luka, Mladena Stojanovi ć a 2, 78000 Banja Luka, Republic of Srpska, Bosnia and Herzegovina
[3]Thermo Fisher Scientific Inc., West Sussex, RH191UB, United Kingdom
[4]Departamento de Física Atómica Molecular y Nuclear, Facultad de Ciencias Físicas, Universidad Complutense, Avda. Complutense s/n, E-28040 Madrid, Spain
[5]Instituto de Matemáticas y Física Fundamental, Consejo Superior de Investigaciones Científicas, Serrano 121, 28006 Madrid, Spain

Abstract

Motivated by its undeniable influence on global warming and ozone destruction, we present joint theoretical and experimental absolute differential cross section for elastic electron scattering from halothane molecule, for incident electron energy of 150 eV.

Introduction

2-bromo-2-chloro-1,1,1-trifluoroethane, commonly known as halothane ($CF_3CHBrCl$), is a multihalogenated derivate of ethane. It is mainly used as an inhalation aneaesthetic. Mostly because of its clinical usage, halothane is widely investigated, but lately, its impact on the environment has motivated further research. Namely, it is known that most of the inhaled aneaesthetics are eliminated from the patient's body without being metabolized, so they are released into the lower atmosphere (Shiraishi et al. 1990). Halothane is known to have a high global warming potential (GWP) (Ishizawa et al. 2011). Its tropospheric lifetime is calculated to be 7 years (Langbein et al. 1999), long enough to reach the stratosphere in considerable quantities. There, halothane can damage the ozone layer, since its ozone depletion potential (ODP), relative to Freon-11, is 1,56 (Langbein et al. 1999), highest among all aneaesthetics. All the above-mentioned give enough motive for research of electron interaction with this molecule.

In this paper, experimental and theoretical results for elastic electron scattering from halothane molecule, for incident electron energy 150 eV are reported. The experiment is performed in crossed beam setting. Relative differential cross section (DCS) is normalized on the absolute scale using the relative flow method, with Ar as a reference gas. The theory is obtained with IAM+SCAR method (Independent Atom Model + Screening Corrected Additivity Rule). A schematic drawing of halothane is shown in Fig. 1.

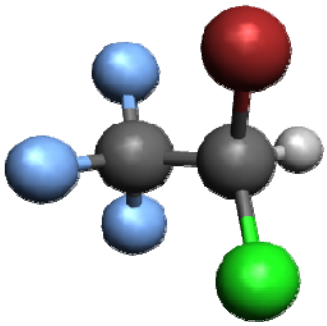

Fig. 1. Schematic drawing of halothane.

Experimental set up

Crossed electron-molecular beam apparatus UGRA which has been described in detail previously by Milosavljevic et al. (2006), was used for measuring absolute differential cross sections for elastic electron scattering on a halothane. The experimental set-up consists of an electron gun (hairpin electron source, up to about 1 μA incident beam current in the energy range from 40-300 eV, a double cylindrical mirror energy analyzer (DCMA) and a channel electron multiplier as a detector. All of these components are enclosed in a double μ–metal shielded vacuum chamber. The incident electron beam is crossed perpendicularly by a molecular beam produced by stainless still needle. The electron gun can be rotated around the needle in the in a limited angular range, from -40° to 126°.The base pressure of about $4x10^{-7}$ mbar was obtained by a turbo-molecular pump. The working pressure was usually less than $5x10^{-6}$ mbar and was checked for each experimental point. The energy resolution is limited by a thermal spread of primary electrons to about 0.5 eV. Halothane was introduced into scattering region from a glass container via a gas line system which was heated (sample container, pipes, needle) to provide stable experimental conditions and to improve the signal. Temperature of the pipes, needle and container were kept at about 40^{o}-50^{o}C. Absolute values for differential cross sections (DCSs) were obtained for 150eV incident electron energy, using relative flow technique (Nickel et al. 1989), at several scattering angles (40^{o} , 70^{o} and 100^{o}). In the relative flow method, the DCS

for scattering of the unknown gas is determined by comparing scattering signals from a standard target (Ar), with its known differential cross sections (Williams 1975), at a given incident electron energy (E_O) and a scattering angle (θ) under identical experimental conditions. To obtain the same profiles for both gas beams, the gases must be operated at pressures behind the needle so that their mean-free paths are the same.

We have taken the gas kinetic diameter for halothane to be 5.6 Å (Lewis et al. 1997). For the present experiment, the ratio of driving pressures (according to their gas-kinetic diameters) is p_{Hal}: p_{Ar}=2.45:1. During the measurement it has been proved by varying the ratio of the halothane and Ar pressures (±15%) that absolute values of the cross sections do not depend significantly.

Analysis and results

Experimentally measured (red circles, for scattering angles from 20° to 110°) and theoretically calculated (black full line, 0°-180°) DCSs, for incident electron energy 150 eV, are shown graphically in Fig. 2. DCS has characteristic behavior for molecular targets, as noticed before (Vukalović et al. 2021). It exhibits a wide minimum at about 90°. Experiment and theory are, in general, in very good agreement, considering absolute scale and shape. Concerning the normalization procedure, described in detail elsewhere (Vukalović et al. 2021), relative flow measurements are shown in Fig. 2. as yellow stars. The reference gas used was Ar, and its absolute DCS values were taken from a paper by Williams and Willis.

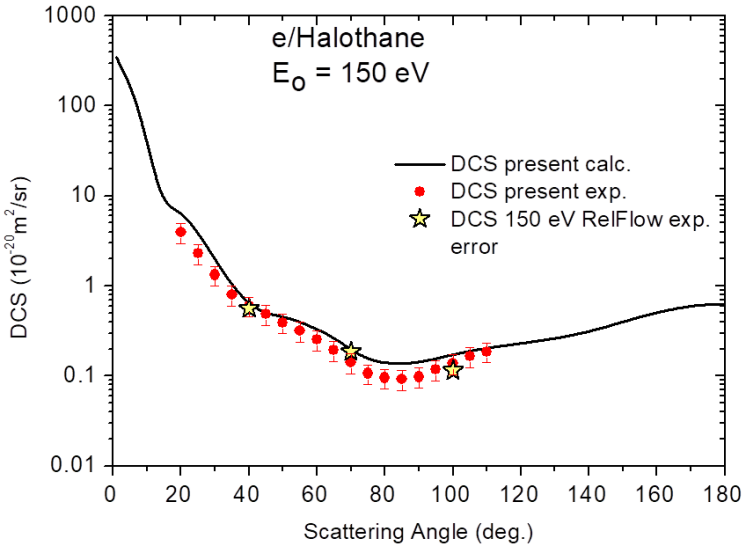

Fig. 2. Angulary dependent differential cross section for elastic electron scattering from halothane molecule, for incident electron energy 150 eV.

Acknowledgments

We acknowledge the financial support of MESTD supplied via Institute of Physics Belgrade. This collaborative work has been undertaken under COST Action CA18212 MD-GAS.

References

Shiraishi, Y., Ikeda, K., 1990, J. Clin. Anesth., 2, 381
Ishizawa, Y., 2011, Anesth. Analg., 112, 213
Langbein, T., Sonntag, H., Trapp, D., Hoffmann, A., et al., 1999, Br. J. Anaesth., 82, 66
Milosavljević, A. R., Mandžukov, S., Šević, D., Čadež, I., Marinković, B. P.: 2006, J. Phys. B: At. Mol. Opt. Phys., 39 609.
Nickel, J. C., Zetner, P. V., Shen, G. and Trajmar, S.: 1989, J. Phys. E :Sci. Instrum., **22,**730
Williams, J. F., Willis, B. A., 1975, J. Phys. B, **8**, 1670
Lewis, D. F. V., Bird, M. G., Parke, V.: 1997, Toxicology, **118,** 92-113.
Vukalović, J., Maljković, J.B., Blanco, F., García, G., et al., 2021, Int. J. Mol. Sci. **23**, 10021
Vukalović, J., Maljković, J. B., Tökési, K., Predojević, B.P. Marinković, 2021, Int. J. Mol. Sci. **22**, 647

Statistics of Management Committee Members from Serbia in COST Actions

Zoran R. Mijić[1] and Bratislav P. Marinković[2]

Institute of Physics Belgrade, Pregrevica 118, 11080 Belgrade, Serbia
[1]E-mail: zoran.mijic@ipb.ac.rs COST National Coordinator (CNC)
[2]E-mail: bratislav.marinkovic@ipb.ac.rs Member of COST Committee of Senior Officials (CSO)

Abstract

COST (European Cooperation in Science and Technology) provides researchers and innovators access to the top scientific and technology networks in Europe and beyond. In order to increase Europe's capacity to solve scientific, technical, and social concerns it connects academics and innovators by providing funding for excellence-driven and multidisciplinary pan-European networks (COST Actions). Each Action is managed by a Management Committee composed of COST Member representatives. In this paper the basic analysis of Serbian representatives in active COST Actions is presented.

Introduction

COST Actions are open, bottom-up networks of researchers and innovators that facilitate pan-European collaboration in a range of scientific and technological domains (Marinković, 2019). COST Action proposals are evaluated on the basis of excellence and can be submitted via an open call procedure. Participants at various stages of their careers collaborate in a field of science and technology of mutual interest to at least seven COST Full Members. The number of countries per Action has increased by 27% in the last seven years, mostly as a result of more Inclusiveness Target Countries (ITCs) joining COST Actions.

COST Action is managed by a Management Committee (Action MC) composed of Action MC Members (COST documents guideline, 2021). The COST National Coordinators (CNCs) is the national contact point in the COST Member responsible for the nomination in the Action MC. The selection of maxima two MC members per Action representing the COST Member state is based on national rules and procedures. Following the good practice, the consultation from Action Main Proposer/Chair prior nomination of MC is required to ensure that the profile of the proposed Action MC Member matches the aims and objectives of the COST Action and, where possible, brings diversity and interdisciplinarity in the Action MC.

An Action starts officially on the date of the first Action MC meeting (MC1) that should take place not earlier than 4 months and not later than 9 months after COST Committee of Senior Officials (CSO - main decision body of COST Association) approval.

Before the start of the Action, nominated persons will automatically become Action MC Members, but after the Action MC1 meeting, new Action MC Members must be validated by the Action MC. Validation occurs implicitly, that is, without any action on the part of the Action MC. An Action MC decision, on the other hand, might clearly approve or reject the nomination. The refusal must be supported by a formal reason submitted within four weeks of the nomination. If no express rejection decision is made within four weeks following nomination, the nomination is confirmed (Annotated Rules for COST actions, 2021).

The Action MC Members should actively participate to the work of at least one Working Group (WG) and represent their COST Member community in order to coordinate the input to the Action and disseminate opportunities arising within the Action at national level. The basic information and data related to the Serbian representatives in active Actions are presented below.

Statistics of MC members from Serbia

The official data obtained by COST Association in May 2022 provide the information on nomination and MC member's statistics for all COST Members (COST statistics, 2022). Fig 1. depicts the average days needed for MC member nomination (for Action secondary proposers) after the official CSO approval. Serbia, with 61 days needed for nomination, is in the middle range with respect to all other countries.

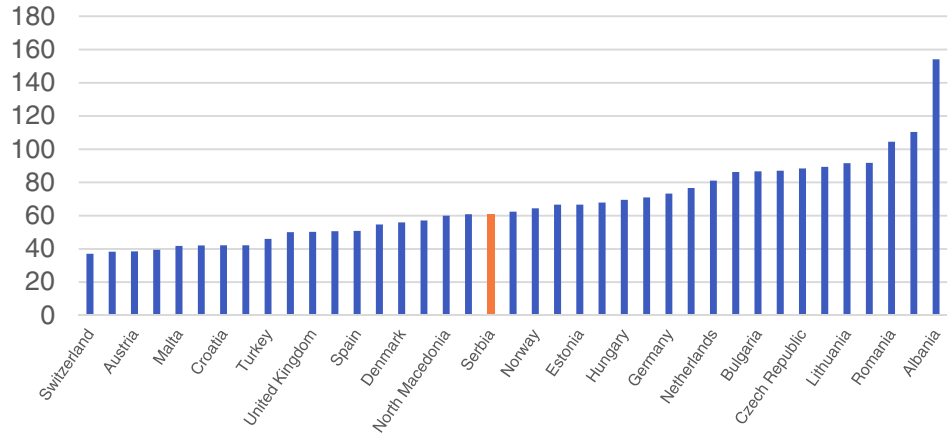

Fig. 1. Days between CSO approval and MC delegate nomination for Actions proposers.

On the other hand 123 days in average is needed for nominations of non-secondary proposers (Fig 2.) indicating the necessity to improve the information sharing on new Actions approval and promotion of benefits for non-secondary proposers to join COST Actions.

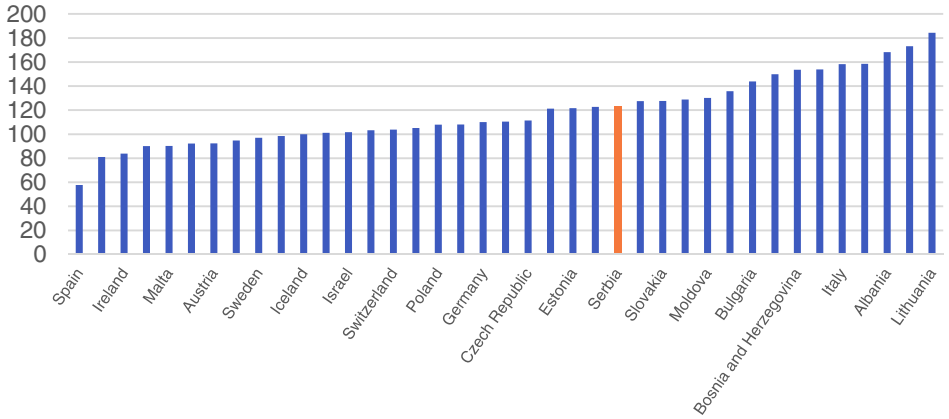

Fig. 2. Days between CSO approval and MC delegate nomination for Actions non-proposers.

The percentage of the nominated MC members at least 1 month before the MC1 meeting is 88.2% for secondary proposers (Fig. 3) and 52.6% for non-proposers (Fig. 4).

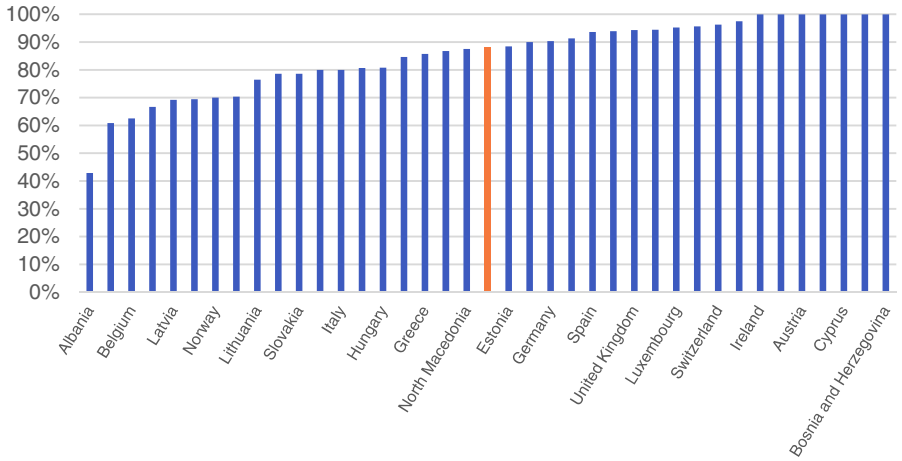

Fig. 3. Percentage of proposers nominated at least 1 month before the first Management Committee meeting.

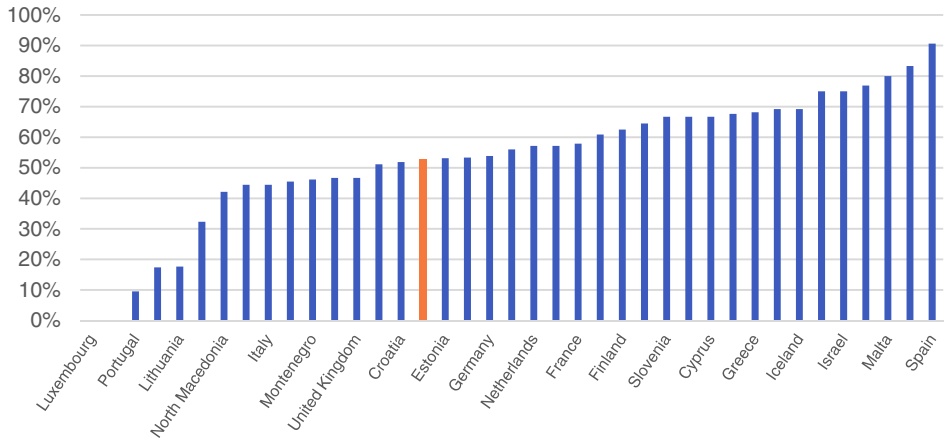

Fig. 4. Percentage of non-proposers nominated at least 1 month before the first Management Committee meeting.

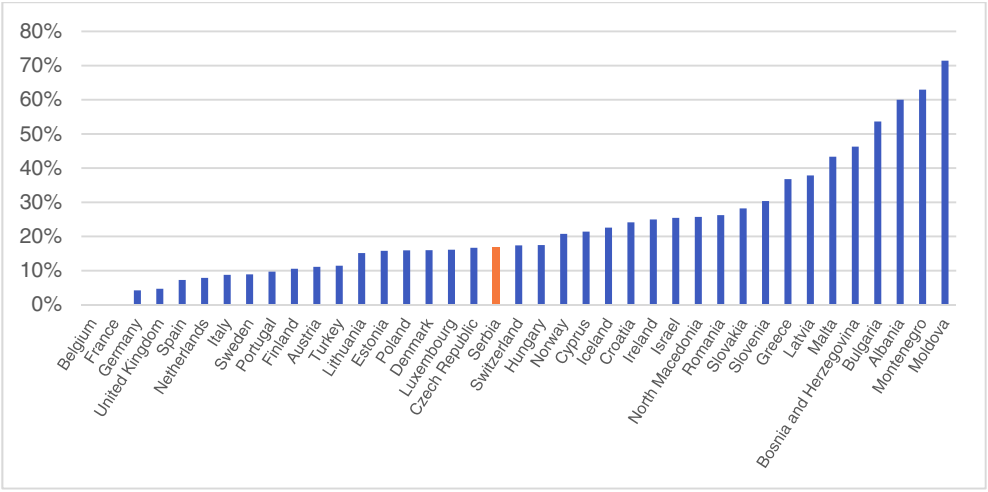

Fig. 5. Percentage of nominated MC Members already active in another Action.

According to the national rule one researcher can participate as MC Member in two active Actions. Such restriction aims to stimulate researcher, especially younger researchers coming from wider scientific community, for joining COST activities by taking one of the leading positions. As a result 16.9% of nominated MC Members are already active in another Action (Fig. 5) allowing pretty high opportunity for other researcher to take an active role. Equal access to leadership

positions, notably with regard to empowerment of young researchers and innovators (researcher or innovator under the age of 40) is one of the key component of The Openness and Inclusiveness COST Principle (The COST Mission, 2021). Serbia, with 46.5% relative mobilization of younger researchers is the leading country in this domain.

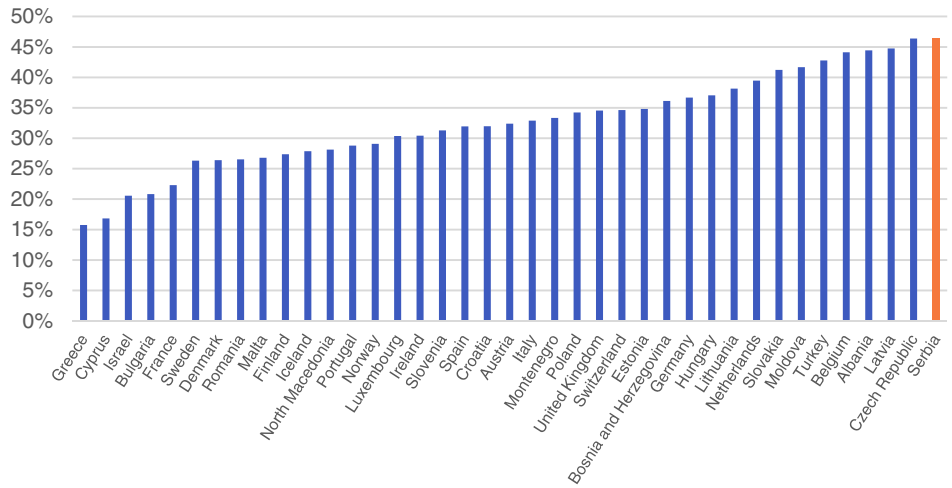

Fig. 6. Relative mobilization of younger researchers.

In addition, gender balance is regarded as an important component of COST's aim to being open and accessible to all categories of researchers. It is consistently emphasized as an essential aspect for COST Actions while organizing their activities. 54.9% of MC members from Serbia are females showing that Serbia reaches pretty fair gender balance (Fig. 7).

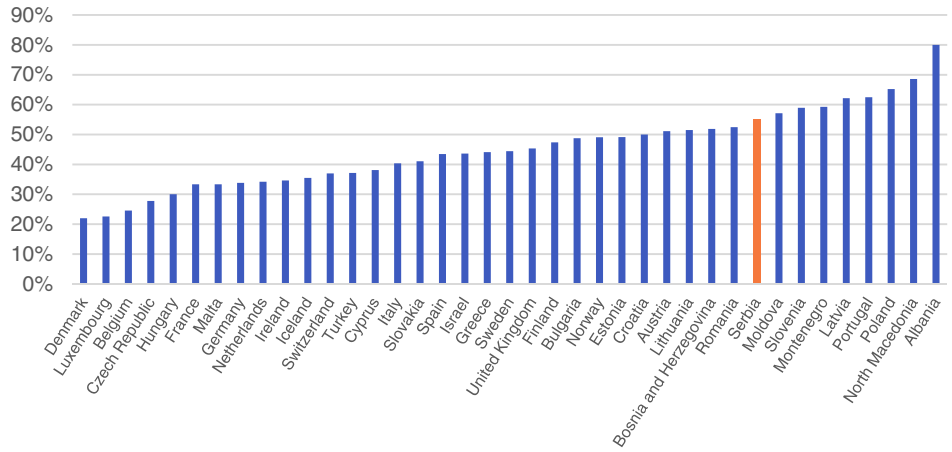

Fig. 7. Percentage of female MC Members.

Conclusions

COST Association provides nomination and MC statistics annually for each country participating in active Actions. Since the nomination procedure and collaborative potential for joining COST Actions are specific for each country there are no common target values which should be achieved, but rather recommendations. The obtained parameters should be useful for national COST office and CNC as indicators what kind of the procedures could be improved in order to attract more participants assuring effective networking activities. Although MC members from Serbia have already significant involvement in COST Actions, national COST office constantly works on improvement of the national nomination procedures. Dedicated national web site and online application form (Serbian COST office, 2022) is expected to further accelerate and facilitate the MC nomination procedure.

Acknowledgments

Thanks are due to The Ministry of Education, Science and Technological Development of the Republic of Serbia and the Institute of Physics Belgrade for national COST office support.

References

Annotated Rules for COST actions (Level C – COST Actions), 2021, available at https://www.cost.eu/uploads/2022/02/COST-094-21-Annotated-Rules-for-COST-Actions-Level-C-2022-02-15.pdf

COST documents guidelines 2021, available a https://www.cost.eu/funding/documents-guidelines/

COST Statistics - Serbia - Participation in COST Activities, Overview 2021 (May 2022).

Marinković, B. P., 2019, "COST Actions as a wide network of researchers and innovators across Europe", Proc. The Seventh Conference on Information Theory and Complex Systems (TINKOS 2019), Belgrade 15-16 October 2019, Book of Abstracts, Eds. Ilić, V. and Mitrović Dankulov, M., Mathematical Institute of the SASA and Institute of Physics Belgrade, University of Belgrade, Serbia

Serbian COST office, 2022, national website available at http://mail.ipb.ac.rs/~ncc-serbia/

The COST Mission, 2021, available at https://www.cost.eu/about/cost-mission/

Collisional and transport processes of low-energy positrons in molecular hydrogen

Saša Dujko[1], Danko Bošnjaković[1], Ilija Simonović[1] and Zoran Lj. Petrović[2]

[1]Institute of Physics Belgrade, University of Belgrade, Pregrevica 118, 11080 Belgrade, Serbia
E-mail: sasha@ipb.ac.rs
[2]Serbian Academy of Sciences and Arts, Knez Mihailova 35, 11001 Belgrade, Serbia

In this work we will give a brief review of positron physics, focusing on the astrophysical processes that positrons undergo in our Galaxy. Several important astrophysical objects are identified as sources of positrons and the physics of positron production and annihilation will be discussed. We discuss in which way the low-energy positron community could help to the positron astrophysics community to make further progress in understanding positron-matter interactions and the matter-antimatter asymmetry problem. As an example, we study the collisional and transport processes of positrons in H_2, which is one of the most abundant molecules in our Galaxy (Prantzos et al. 2011, Banković et al. 2012).

We apply a multi term theory for solving the Boltzmann equation and Monte Carlo simulation technique (Dujko et al. 2010) to investigate various aspects of positron transport in H_2 under the influence of electric and magnetic fields crossed at arbitrary angles. The hierarchy resulting from a spherical harmonic decomposition of the Boltzmann equation in the hydrodynamic regime is solved numerically by representing the speed dependence of the distribution function in terms of an expansion in generalized Laguerre polynomials about a Maxwellian velocity distribution at an internally determined temperature. Positron transport properties, including mean energy, drift velocity and diffusion tensor, are calculated over a range of reduced electric and magnetic fields, and angles between the fields. The rate coefficient for positronium (Ps) formation is also calculated and compared with other rate coefficients. It is found that the difference between the two sets of transport coefficients, the bulk, and the flux, resulting from the explicit effects of Ps formation, can be controlled either by the variation in the magnetic field strengths or by the angles between the fields. Special attention is given to the synergistic effects of Ps formation and angle between the fields on the phenomenon of negative differential conductivity (Banković et al. 2009). In addition, it is found that the off-diagonal elements of the diffusion tensor can have magnitudes of an

equivalent order of the diagonal elements suggesting consideration is required for their inclusion into prospective models of positron traps.

Among many interesting phenomena we note the existence of runaway positrons in H_2. This raises a question: Is a set of cross sections for the scattering of positrons in H_2, used as input to solve the Boltzmann equation, complete? To resolve this issue and as a first step, we investigate the influence of rotational excitation on positron transport for the lower values of the applied electric fields. The cross sections for rotation excitations are calculated assuming the Gerjuoy-Stein and Dolgarno-Moffett theories (Natisin et al. 2014). As a curiosity, we note that in this work we present the variation of the third-order transport coefficients for positrons with the applied fields for the first time.

In the final segment of this work, we will discuss our Monte Carlo models of a Penning-Malmberg-Surko positron trap (Fajans and Surko, 2020). It will be shown that positrons begin to move from a beam-type distribution and thermalize to an isotropic Maxwellian distribution at a given temperature. Simulation results will be displayed for a range of trap settings, including those using mixtures of N_2 and CF_4, pure CF_4 and pure H_2. We will illustrate the high efficiency of a positron trap that uses pure CF_4 using advanced Monte Carlo modeling and physical arguments (Marjanović et al. 2016).

References

Prantzos, N., Boehm, C., Bykov, A. M., et al. 2011, RvMP, 83, 1001

Banković A., White R. D., Buckman S. J., Petrović Z. Lj., 2012, Nucl. Instrum. Meth. Phys. Res. B., 279, 92

Dujko S., White R. D., Petrović Z. Lj., Robson R. E., 2010, Phys. Rev. E 81, 046403

Banković A., Petrović Z. Lj., Robson R. E., Marler G. P., Dujko S., Malović G., 2009, Nucl. Instrum. Meth. Phys. Res. B., 267, 350

Natisin M. R., Danielson J. R., Surko C. M., 2014, J. Phys. B: At. Mol. Opt. Phys., 47, 225209

Fajans J., Surko C. M., 2020, Phys. Plasmas, 27, 030601

Marjanović S., Banković A., Cassidy D., Cooper B., Deller A., Dujko S., Petrović Z. Lj., 2016, J. Phys. B: At. Mol. Opt. Phys., 49, 215001

The usage of perception, feed and deep feed forward artificial neural networks on the spectroscopy data

N. M. Sakan, I. Traparić, V. A. Srecković and M. Ivković

Institute of Physics Belgrade, Pregrevica 118, 11000 Belgrade, Serbia
E-mail: nsakan@ipb.ac.rs

The usage of machine learning algorithms is a growing field of research. Since the computer power is constantly growing its application is often found in a wide variety of applications from determination of objects on a photograph all the way to expert systems capable to determine adequate states and predicted outcomes of complex systems, from difficult to maintain machines up to the assistance in human health monitoring. Application of the artificial neural networks has fall into focus of our interest because of the flexibility of their applications as well as a variety of complex problems that have been solved with their application. All the mentioned has been a decision factor for the applying of neural networks for the decision process of determining a stellar spectral type as a example of application on astrophysical data.

The usage of systems related to the functions of the neural networks has been in focus of investigation since mid-1940 (McCulloch, et al. 1943), but the real usage has evolved with the application of modern days digital computers, that enabled a construction of networks of enlarged complexity. One of the simplest neural networks, that could be seen more as a test case of validity of operation of artificial intelligence systems is perceptron (Rosenblatt, 1958).

The prediction as well as sensitivity on the training dataset is in favor of more complex networks and is primary goal of our investigation of their application on spectral datasets and measurements.

As a consistent base the set of easily readable, open access data a choice was made on files for the 131 stellar spectra published by A. Pickles (A.J. Pickles, 1998) (available at accompanying reference appended to the bibliographical entry, as seen in May 2022)

The results are promising and the further research on the field is expected. The quality of the trained artificial neural network prediction is related to the dataset as well as its structure, an effort on large scale database for the machine learning as well as finding a promising field of application should be carried out.

Acknowledgements

The research was funded by the Ministry of Education, Science and Technological Development of the Republic of Serbia, Contract: 451-03-68/2022-14/200024 and supported by the Science Fund of the Republic Serbia, NOVA2LIBS4fusion Grant no. 3108/2021

References

McCulloch, Warren; Walter Pitts (1943). Bulletin of Mathematical Biophysics. **5**, 115.
Rosenblatt, F. (1958). Psychological Review. **65,** 386.
Pickles, A.J. (1998) Publications of the Astronomical Society of the Pacific **110**, 863.

Stark broadening method of Hydrogen Balmer beta for low-density atmospheric pressure discharges

Nikola Cvetanović[1] and Bratislav M. Obradović[2]

[1]Faculty of Transport and Traffic Engineering, 11000 Belgrade, Serbia
E-mail: nikola@ff.bg.ac.rs
[2]University of Belgrade, Faculty of Physics, 11001 Belgrade, Serbia

In recent years there has been a growing demand for measuring the electron density in atmospheric pressure discharges suitable for application. Such data is crucial for modeling and reactor optimization. These discharges include volume dielectric barrier discharges, surface barrier discharges, low temperature plasma jets, RF discharges with bare electrodes or covered by dielectric. However, here measurement of plasma density using spectroscopic methods poses a difficult task, since all such plasma is of low to mid density. Therefore, the nonhydrogenic atomic lines spectra cannot be used and the only option are the hydrogen lines, mostly Balmer beta and gamma. Fortunately, in atmospheric pressure plasma hydrogen is always present in traces, and Balmer lines are strong enough to be employed, see for example Cvetanović et al. 2018.

The H_β line is commonly used to obtain electron density due to its advantages of strong Stark broadening dependence on electron density, and weak sensitivity to electron temperature. However, its broadening can only be applied in the case of considerably high electron density ($>10^{20}$ m^{-3}) making it difficult to apply to many types of low temperature plasma, N. Konjević et al. 2012. Using the classical Voight fit below this value may lead to significant error and uncertainty. Therefore, a fine-structure fitting method must be applied to get more accurate results. This fitting method is based on assuming that the broadening mechanism of H_β line also applies to the 7 fine-structure components. This method has been used by Hoffman et al. 2011, to analyze the electron density in atmospheric pressure RF plasma jet. Palomares et al. 2012 experimentally validated the applicable range of this method down to $6 \cdot 10^{18}$ m^{-3} by comparing it to an independent method - Thomson scattering.

In the fine-structure fitting, Stark broadening is calculated by assigning a Voigt shape to each fine component. The overall profile is then analyzed by convoluting separate fine structure transitions of H_β as line profiles, with relative line strengths and line shifts being the same as in the zero-field case. Due to the low plasma density, this may be taken as a valid assumption. In other words, each fine-structure transition is assigned with its corresponding Doppler, Van der Waals, Stark broadening, and instrumental broadening so that the overall profile is

obtained as a superposition of profiles. In this approach, the same Stark width which is expected from theory for the entire line, is assigned to each fine-structure component. The fine-structure fitting can be used to improve the accuracy of electron density calculation close to the threshold of classical method, but above all for checking the validity of the obtained results for plasma density in the conditions when Van der Waals broadening is below the fine-structure limit of 0.05 nm.

Examples of method application are shown in two experiments with atmospheric pressure helium discharges, Wang 2020. The fine-structure fit was compared with results from a simple Voigt fit.

References

Cvetanović N., Oleksandr G., Petr S., Zemánek M., Antonín B., Tomáš H., ,2018, Plasma Sources Sci. Technol. 27 025002

Hofmann S., van Gessel A. F. H., Verreycken T., and Bruggeman P., 2011, Plasma Sources Sci. Technol. 20, 065010

Konjević N., Ivković M., and Sakan N., 2012, Spectrochim. Acta Part B 76, 16

Palomares J. M., Hübner S., Carbone E. A. D., de Vries N., van Veldhuizen E. M., Sola A., Gamero A., and van der Mullen J. J. A. M., 2012, Spectrochim. Acta Part B 73, 39

Reader J., 2004, Appl. Spectrosc. 58, 1469

Wang L., Cvetanović N., Obradović B.M., Eusebiu-Rosini I., Dinescu G., C. Leys, A. Nikiforov, 2020, Jpn. J. Appl. Phys. 59 SHHB01

History of Serbian involvement in LSST

Darko Jevremovic

Astronomical Observatory, Volgina 7, 11060 Belgrade 38, Serbia

I will first describe Rubin/LSST and summarize the Serbian involvement in LSST since 2010. In kind contribution of Serbian Technical group (STG) is already recognized and I will point toward possible further contributions of STG to Rubin operations.

On the Stark broadening parameters of Ir II spectral lines

Zoran Simić[1] and Nenad Sakan[2]

[1]Astronomical Observatory, Volgina 7, 11060 Belgrade, Serbia
E-mail: zsimic@aob.rs
[2]University of Belgrade, Institute of Physics, PO Box 57, 11001 Belgrade, Serbia

The presence of singly ionized Iridium lines in spectra of chemically peculiar stars (CP stars) is experimentally confirmed recently. Stark widths for additional 50 Ir II spectral lines are calculated using the modified semi-empirical method of Dimitrijević and Konjević. The calculations of Stark widths (FWHM) for electron-impact broadening, have been performed for a perturber density of 10^{17} cm^{-3} and for a temperature value of 10000K. In order to have a easier to monitor and observe atomic data for spectroscopy the transitions in our table follows the list of spectral lines from the NIST database.

Within the frame of the presented work a additional data for 50 more Ir II spectral lines are added to the previously calculated data of 301 lines presented earlier (Simić et al. 2021.). The enhanced dataset is applicable to the describing of CP stars spectra and is step forward towards the completing of dataset for known CP stars atmosphere composition.

References

Zoran Simić, Nenad M. Sakan, Nenad Milovanović, and Mihailo Martinović. Singly ionized iridium spectral lines in the atmosphere of hot stars. International Astronomy and Astrophysics Research Journal, 3(2): 33-47, 2021; Article no. IAARJ.70329

Review of atmospheric aerosol optical properties profiling and lidar station activities in Serbia

Zoran Mijić[1], Maja Kuzmanoski[1], Luka Ilić[1,2], Aleksander Kovačević[1] and Darko Vasiljević[1]

[1]Institute of Physics Belgrade, Pregrevica 118, 11080 Belgrade, Serbia
E-mail: zoran.mijic@ipb.ac.rs
[2]now at Barcelona Supercomputing Center, Plaça Eusebi Güell, 1-3, 08034 Barcelona, Spain

Abstract

An advanced laser remote sensing technique – LIDAR (Light Detection And Ranging) is the most appropriate tool for providing range-resolved atmospheric aerosol vertical distribution. LIDAR measurements of aerosol optical properties with high spatial and temporal resolution give detailed information on the occurrence and development of aerosol structures. In this study a brief introduction of a lidar system developed at the Institute of Physics Belgrade in the past and the new system currently operating, is presented together with several activities conducted within European lidar network. The capacity and the experience from measurement campaigns aiming to provide near real time data products and study the changes in the atmosphere is also discussed.

Introduction

Clouds and atmospheric aerosols play an important role in the Earth's radiation budget, thus quantifying the role of aerosols in climate system is crucial for better weather forecasting and understanding climate change. The amount of scattered and absorbed radiation (both incoming solar and outgoing terrestrial) varies according to aerosol composition, size and shape distributions. The short lifetime and large variability in space and time further contribute to the identification of aerosol radiative forcing as one of the significant unknowns in our understanding of climate change (Stocker et al., 2013). The complexity of the aerosol interaction with the climate system makes it necessary to estimate its impact through the integrated use of ground-level and airborne *in-situ* measurements, ground-based remote sensing, and space-borne observations in combination with advanced numerical modelling. LIDAR (Light Detection And Ranging), an active remote sensing technique, has proved itself to be the optimal tool for profiling height-

resolved atmospheric aerosol optical parameters. Various aerosol lidar techniques have been developed during the last several decades like backscatter lidar, Raman lidar, depolarization lidar, and high spectral resolution lidar. Each type of lidar can operate at one or multiple wavelengths. The LIDAR principle is based on laser emission of short-duration light pulses into the receiver field of view. The intensity of the light backscattered by atmospheric molecules and particles is measured versus time (through the telescope receiver, collimating optics, a bandpass filter for daylight suppression) by an appropriate detector. The signal profile is recorded by an analog-to-digital converter or by a photon-counting device and accumulated for a selected integration period, which may range from a few to thousands of individual laser shots – spanning time intervals from seconds to minutes. In order to establish a comprehensive and quantitative statistical data base of the horizontal and vertical distribution of aerosols at European scale the lidar network called EARLINET (the European Aerosol Research LIdar Network) was founded in 2000 (Pappalardo et al., 2014). The development of the quality assurance strategy, the optimization of instruments and data processing, and the dissemination of data have contributed to significant improvement of the network towards a more sustainable observing system. Currently, EARLINET contributes to the Aerosol, Clouds and Trace gases Research Infrastructure (ACTRIS), the pan-European research infrastructure producing high-quality data and information on short-lived atmospheric constituents. In this paper a brief review of atmospheric aerosol remote sensing capacity over the past period at the Institute of Physics Belgrade (IPB), Serbia, is presented together with short introduction on the methodology of elastic backscatter and Raman lidar systems. In addition, experience from several activities of IPB lidar station from dedicated measurement campaigns is described.

Methodology

The lidar equation for return signal $P(\lambda)$ elastically backscattered by air molecules and aerosol particles is found to be

$$P(\lambda,r) = P_0(\lambda) C \frac{O(r)}{r^2} \beta(\lambda,r) \exp\left[-2\int_0^r \alpha(r')dr'\right] \qquad (1)$$

where $P_0(\lambda)$ is the laser pulse power; C is a system constant (taking into account the optics and electronics used); $O(r)$ denotes the unitless correction function that corrects the lack of coincidence of the laser beam and the receiver field of view for ranges below the complete overlap height; r is the distance between the laser exit and the point of scattering in the atmosphere; $\alpha(\lambda,r)$ and $\beta(\lambda,r)$ denote the height (distance) and wavelength (λ) dependent extinction and backscatter coefficients respectively. The extinction coefficient describes the ability of particles to scatter or absorb light at a given wavelength while the backscatter coefficient (scattering coefficient at 180°, normalized to the unit solid angle) refers only to scattering events. Backscattering and extinction are both caused by particles and molecules.

While the molecular scattering properties can be determined with sufficient accuracy from the available measurements of temperature and pressure profiles, the aerosol backscatter $\beta_a(\lambda,r)$ and extinction $\alpha_a(\lambda,r)$ coefficients remain to be retrieved. In lidar profiling, the most significant errors occur during signal inversion, when the optical parameters of the atmospheric aerosols are extracted from the lidar signals using a number of implicit premises and *a priori* assumptions. Two *a priori* assumptions are necessary to allow the retrieval of $\alpha_a(\lambda,r)$ and $\beta_a(\lambda,r)$ profiles from the elastic lidar measurement*:* an assumed value of the lidar ratio (aerosol extinction/backscatter value) and the reference range chosen such that the particle backscatter coefficient is negligible compared to the known molecular backscatter coefficient value. The main drawback of this method is the fact that the extinction profile is estimated from the determined backscatter coefficient profile.

The first elastic backscatter lidar system at the IPB was developed in 2008 as bi-axial lidar system with transmitter unit based on a water-cooled, pulsed Nd:YAG laser, emitting pulses of 100 mJ and 50 mJ output energy at 1064 and 532 nm respectively, with a 20 Hz repetition rate (Fig .1). The optical receiver was the Schmidt–Cassegrain telescope with a primary mirror of 304.8 mm diameter. Si PIN photodiode FD5N was used to detect elastic backscatter lidar signal at 532 nm. An interference filter with 3 nm bandwidth was used to select the lidar wavelengths and to reject the atmospheric background radiation during daytime operation. For analog detection, the signal was amplified according to the input range selected and digitized by an A/D converter NI5124.

Fig. 1. Elastic backscatter lidar system developed at IPB.

The described system was the first lidar system of that kind used for aerosol profiling in Serbia. To overcome the limitation of elastic backscatter lidar technique the so-called Raman lidar technique can be used and the profile of particle extinction coefficient can directly be determined. Raman lidar measures lidar return signals elastically backscattered by air molecules and particles and inelastically (Raman) backscattered usually by nitrogen molecules. Whereas the

elastic backscatter lidar is operational both at day and night, the Raman lidar is mainly used during nighttime, due to the strong daylight sky background. The determination of the particle extinction coefficient from molecular backscatter signals is rather straightforward since neither lidar ratio nor other critical assumptions are needed (Kovalev, 2015).

Fig. 2. IPB Raman EARLINET joining lidar station.

In 2014 Raman lidar operating at 355 nm and 387 nm (N_2) was set up at IPB, establishing Serbian EARLINET joining lidar station (Fig. 2). The basic characteristics of IPB Raman lidar are summarized in Table 1.

Table 1. IPB Raman lidar system components

Emitter		Receiver	Detection Unit
Pulse laser source:	Nd:YAG (Quantel CFR200)	Telescope type: Cassegrain, model Raymetrics DK250	LICEL TR20-160 (12 bit at 20 MS/s), 250 MHz fast photon
Wavelength	1064, 532, 355 nm	Telescope aperture: diameter: 250 mm	Detectors: Photomultiplier Tubes (Licel-Hamamatsu-R9880U-110)
Energy/pulse	105/45/65 mJ	Field of view:0.5- 3 mrad (variable)	Detection mode: Analog and photon counting
Pulse duration and repetition	5 ns 20 Hz	Fieldstop type: Circular - Iris Diaphragm, 3mm user selectable	Spatial resolution (raw): 7.5 m
Laser beam diameter:	15 mm (expanded)	Elastic wavelength 355 nm	Full overlap: 250 m
Laser beam divergence:	0.33 mrad	Raman wavelength: 387 nm (N_2)	Effective range: 0.05 – 16 km

As a joining lidar station, systematic aerosol profiling has started in 2014 mostly for providing data for potential climatological studies as well as conducting dedicated measurements during Saharan dust intrusions or assessment of planetary boundary layer evolution (PBL) (Ilić et al., 2018). An example of such measurement performed on February 19, 2014 is presented in Fig 3. together with aerosol backscatter coefficient profile retrieved and dust load simulated by Dust REgional Atmospheric Model (DREAM) (Ničković et. al, 2011).

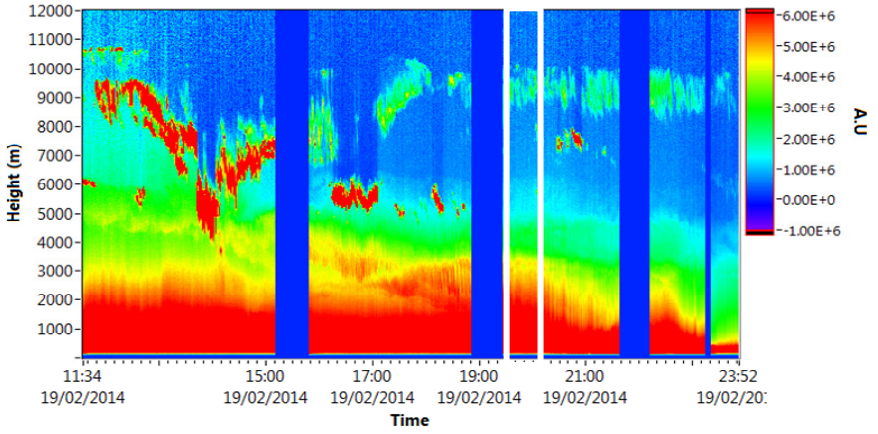

Emission wavelength: 355 nm Detection wavelength: 355 nm
Detection mode: an+pc, Temporal resolution: 60 s, Spatial resolution:

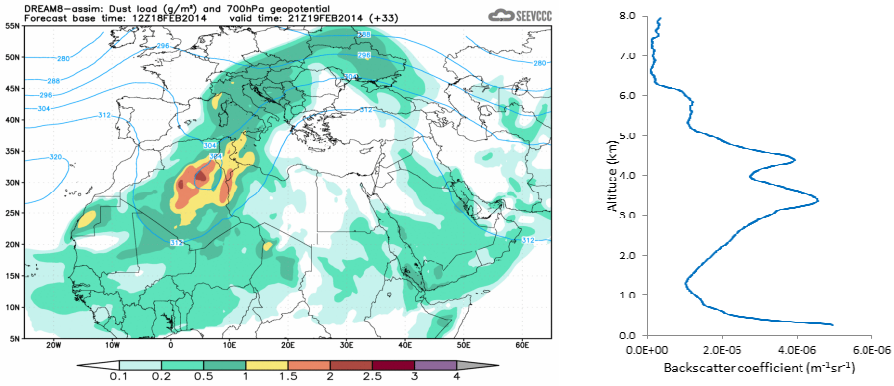

Fig. 3. LIDAR range corrected signal (above) and dust load over South Europe estimated by the DREAM model (below, left) on February 19, 2014; backscatter coefficient profile (below, right) retrieved for the selected time period (white rectangle).

Activities of the IPB lidar station

In addition to regular aerosol profiling mostly performed at the very beginning after official joining the lidar network, several studies were conducted related to the application of gradient method for the identification of aerosol layer, as well as the evolution of PBL height (Ilić et al., 2018). The IPB lidar station also actively participated in several measurement campaigns organized through the EARLINET network.

The EUNADICS-AV experiment for NRT alerts

Following the existing needs, the methodology providing a tailored aerosol products for aviation hazards based on high-resolution lidar data was developed with the aim to provide the EARLINET early warning system (EWS) for the fast alerting of airborne hazards (Papagiannopoulos et al., 2020). The application of the EWS and the timely delivery of the EARLINET data were tested in real time during the EUNADICS-AV exercise in March 2019. Each station submitted raw lidar data to the Single Calculus Chain (SCC) server every hour, which were automatically available on the EARLINET Quicklook Interface (https://quicklooks.earlinet.org/, last access: May 2022). The SCC is a tool created inside the EARLINET network for the automatic analysis of aerosol lidar observations (D'Amico et al., 2015). The primary goal of SCC is to offer a data processing chain that allows all EARLINET stations to retrieve aerosol products like backscatter and extinction profiles (measures of aerosol load) completely automatically. The raw lidar data were processed in less than 30 min after the measurement, enabling the timely delivery of the lidar data and the tailored product. When the raw data was submitted to the SCC server, it was instantly processed and made publicly available through the EARLINET portal in order to launch the alert distribution. The exercise revealed the network's strength, which, if activated immediately, can permit measurements in the event of natural threats for aviation.

COVID-19 Campaign

A dedicated EARLINET measurement campaign was organized as part of the ACTRIS initiative to study the changes in the atmosphere during the COVID-19 lockdown period in May 2020, in order to monitor the atmosphere's structure during the lockdown and early relaxation period in Europe, and to identify possible changes due to decreased emissions by comparison to the aerosol climatology in Europe. The EARLINET near real time functioning was proven throughout the campaign, based on earlier experience from the EUNADICS-AV exercise. The IPB lidar station, along with 21 EARLINET stations, participated in the campaign by providing vertical aerosol profiles twice per day (minimum two hours

measurements at noon, and minimum two hours after sunset). The measurements were submitted and analyzed in near-real time by SCC. The first analysis was based on the data processed by the SCC and directly published on the THREDDS server in NRT. The preliminary analysis made on aerosol lidar data shows that simple comparison of the observed backscatter values with the climatological values from 2000-2015 is not sufficient to extract a clear conclusion on how much the COVID-19 lock-down has impacted the aerosols in the atmosphere, but a certain effect in the lower troposphere can be seen.

Conclusions

Lidar systems are optimal tools for providing range-resolved aerosol optical parameters and information on the atmospheric structure. The IPB lidar station is the only lidar station for aerosol profiling in Wester Balkans matching EARLINET quality control and quality assurance requirements. A brief description of the station capacity and activities in a few measurement campaigns are presented. Beyond the scientific goals of these campaigns, the actions organized by EARLINET/ACTRIS (NRT delivery of the data and fast analysis of the data products) proved that aerosol lidars are useful for providing information not only for climatological purposes, but also in emergency situations. Although the IPB lidar station is able to provide valuable data, automatization of the measurement process and the upgrade to the multiwavelength lidar system are required.

Acknowledgments

The authors acknowledge funding provided by the Institute of Physics Belgrade, through the grant by the Ministry of Educations, Science, and Technological Development of the Republic of Serbia. The financial support for EARLINET in the ACTRIS Research Infrastructure Project by the European Union's Horizon 2020 research and innovation programme under grant agreement No. 654109 and previously under the grants No. 262254 in the 7th Framework Programme (FP7/2007-2013) and no 025991 in the 6th Framework Programme (FP6/2002-2006) is gratefully acknowledged.

References

D'Amico, G., Amodeo, A., Baars, H., Binietoglou, I., Freudenthaler, V., Mattis, I., Wandinger, U., and Pappalardo, G., 2015, Atmos. Meas. Tech., 8, 4891-4916.

Freudenthaler, V., 2008, Proceedings of 24th International Laser Radar Conference, 23-27 June, Boulder, USA

Ilić, L., Kuzmanoski, M., Kolarž, P., Nina, A., Srećković, V., Mijić, Z., Bajčetić, J., Andrić, M., 2018, J.Atmos.Sol.-Terr. Phys.,171,250-259.

Kovalev, V. A., 2015, Solutions in lidar profiling of the atmosphere, John Wiley & Sons, Inc.

Ničković, S., Kallos, G., Papadopoulos, A., and Kakaliagou, O., 2001, J. Geophys. Res., 106, 18113- 18130.

Nicolae, D., Mona, L., Amodeo, A., D'Amico, G., Freudenthaler, V., Pietras, C., Baars, H. et.al. 2020, EARLINET/ACTRIS analysis of aerosol profilesduring the COVID-19 lock-down andrelaxation period -A preliminary study on aerosol properties in the low and high troposphere, Report, https://www.earlinet.org/index.php?id=covid-19-reports

Papagiannopoulos, N., D'Amico, G., Gialitaki, A., Ajtai, N., Alados-Arboledas, L., Amodeo, A., Amiridis, V., Baars, H., Balis, D., Binietoglou, I., Comerón, A., Dionisi, D., Falconieri, A., Fréville, P., Kampouri, A., Mattis, I., Mijić, Z., Molero, F., Papayannis, A., Pappalardo, G., Rodríguez-Gómez, A., Solomos, S., and Mona, L., 2020, Atmos. Chem. Phys., 20, 10775–10789.

Pappalardo, G., Amodeo, A., Apituley, A., Comeron, A., Freudenthaler, V., Linné, H., Ansmann, A., Bösenberg, J., D'Amico, G., Mattis, I., Mona, L., Wandinger, U., Amiridis, V., Alados-Arboledas, L., Nicolae, D., and Wiegner, M., 2014. Atmos. Meas. Tech., 7, 2389–2409.

Stocker,T. F., Qin D., Plattner,G.-K.Tignor, M., Allen,S. K., Boschung,J., A. Nauels, Xia,Y., Bex V., Midgley,P. M., 2013, IPCC: The Physical Science Basis, Contribution of Working Group I to the Fifth Assessment Report of the Intergovernmental Panel on Climate Change, Cambridge University Press, Cambridge, United Kingdom and New York, NY, USA.

Laser spectroscopy and magnetic resonance atomic magnetomerty in search for dark mater: New bounds on Axion like dark matter from GNOME network of OPM's

Saša Topić, and Zoran D. Grujić

Institute of Physics, Center for Photonics, Pregrevica 118, 11080 Belgrade, Serbia

Contact: Saša Topić (stopic@ipb.ac.rs)

Abstract. In this work we present newest results from the science Run 5 of Global Network of Optical Magnetometers for Exotic physics (GNOME) presented in. Long uninterrupted time series and novel pre-processing methods provide more stringent bounds that are used to estimate exclusion domain of mass and interaction strength of hypothetical axionic or axion like dark matter in form of topological defects. Hypothetical axions or Axion Like Particles (ALP's) are form of ultralight bosonic matter that are postulated in order to solve strong CP problem and matter-antimatter imbalance in the Universe [1] [2]. This type od Dark Matter (DM) has a number of detectable signatures, one being in form of axionic field coupling to fermions that results in formation of pseudo-magnetic fields during passage through topological defect. The GNOME experiment described in [5] and [6] is designed as GPS referenced worldwide distributed network of quantum cross-correlated sensors that increases its sensitivity reach and excludes false positives. Science Run 5 lasted from 24. August to 26. October of 2022 and included, at the highest extent, 11 stations and is characterized by lowest amount of noise, optimal station placement and highest quality of data compare to previous Science Runs [3]. Novel scheme for measuring bandwidth of each station and its frequency response was devised along with pulse sequences that made possible re-scaling in order of site-specific coupling of Optically pumped magnetometers (OPM) to magnetic perturbation as presented (Fig. 1). We present various sensors in the GNOME network and will give other potential uses of data collected by the network.

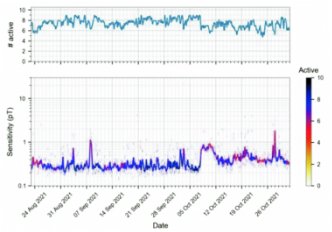

Figure 1: Representation of number of active sensore over time (upper frame); representation of rescaled magnetic field sensitivity of entire network (lower frame).

REFERENCES

[1] D. Budker and M.V. Romalis, *Nat. Phys*., **23** (2007), 229
[2] M. Pospelov, et al., *Phys. Rev. Lett.* **110** (2013), 021803
[3] S. Afach et. *Nature Physics*. **17** (2021), 1396-1401
[4] S. Afach et al. *Physics of The Dark Universe.* **22**, (2018), 162
[5] Pustelny et al., *Ann. Phys.* **525** (2013), 659-670
[6] M.P. Ledbetter, M.V. Romalis and D.F. Jackson Kimball, *Phys. Rev. Lett.* **110** (2013), 040402

SECTIONS (MINI PROJECTS)

S1 Radiative Processes and Spectra

S2 Spectral line profiles in stellar and laboratory plasmas

S3 A&M DATA and HPC

S4 A&M DATA and standards

S5 Modeling the Atmosphere: data&models

S6 COST

AUTHORS' INDEX